2006:53

LICENTIATE THESIS

L

TM-Rolling of Heavy Plate and Roll Wear

Mikael Jonsson

Luleå University of Technology
Department of Applied Physics and Mechanical Engineering
Division of Material Mechanics

2006:53 | ISSN: 1402-1757 | ISRN: LTU-LIC -- 06/53 -- SE

TM-rolling of Heavy Plate and Roll Wear

MIKAEL JONSSON

Division of Material Mechanics
Department of Applied Physics and Mechanical Engineering
LULEÅ UNIVERSITY OF TECHNOLOGY
Luleå, Sweden, 2006

Abstract

The heavy plate rolling process needs accurate predictions of the process parameters. The plate thickness, flatness and rolling stability are of this direct influenced as well as the productivity. Therefore, careful calculation of the process parameters and pass schedules is necessary. The thesis is concerned with two aspects of controlling rolling; the choice of optimal pass schedules and roll wear.

A software has been developed in Paper A to determine optimal pass schedules for thermomechanical rolling in order to obtain a fine microstructure. It includes models of the effect of strain, precipitates, static and metadynamic recrystallization and austenite grain size on the final grain size. The predicted grain sizes for four different cases were compared with experimental results. It was also used to study the effect of different delay times during the pass schedule of rolling thermomechanical plate. The results show that an increase in delay times results in finer ferrite grains are received. The refinement is however small for long delay times. Long delay times also affect the productivity negatively.

A method for modeling of the work roll contour in a four high mill is presented in Paper B. The active parameters were found to be the plate length and the variations of the pressure from the plate and the back-up roll on the work roll along the work roll barrel. The method is build up with statistical methods. The bases for the statistics are simulations of different rolling cases and measurements from the production of heavy plates in Oxelösund. The proposed wear contour model was found to be in good agreement with the measurements from the production.

Keywords: Heavy plate, thermomechanical rolling, roll wear modeling

Preface

This thesis was performed in the national graduate school for metal forming. The work was financially supported by SSAB Oxelösund, the Swedish Foundation for Knowledge and Competence Development (KK-stiftelsen), Jernkontoret and Dalarna University.

Mikael Jonsson
Oxelösund, August 2006

Thesis

This thesis consists of an overview and the following appended papers:

Paper A
An investigation of different strategies for thermo-mechanical rolling of structural steel heavy plates
Mikael Jonsson
Published in ISIJ International, Vol.46, No. 8, 2006

Paper B
Modeling work roll wear in a four-high mill
Mikael Jonsson
Submitted to Journal of Steel Research International, April 2006

Contents

1 Introduction

The hot rolling process of high quality heavy plates requires accurate predictions of process parameters. Some of these models are used on-line and must therefore be carried out as fast and accurate as possible. These demands presuppose explicit models that can be handled with as little iteration as possible. Hot rolling involves large forces on the rolling equipment and causes stresses and deformations in it. Moreover, the shape of the rolled material is directly influenced of the deformation in the mill. A deviation in the precalculated process parameters may lead to worsen product quality or even an expensive break down. In other words, there is a great need of accurate on-line models in a heavy plate mill.

The focus on the research project has been development of new strategies and methods for complicated parts of the rolling. The procedure has been a mix of literature studies, computer simulations and full size experiments.

1.1 Aim of current work

The aim of this work was to investigate new models and strategies in order to improve both the quality and the productivity in the mill. The research question is formulated as:
How can the rolling be modeled and controlled?
The work has been limited to the following parts in the current licentiate thesis:

- Investigation of how different pass schedules influence the microstructure in thermomechanical rolling.
- Simulation of the work roll wear contour after a high number of passes.

2 The production at SSAB Oxelösund

Heavy plates are produced at SSAB Oxelösund. Increasing costs for fuel and energy is driving the interest for lightweight constructions made of extra and ultra high strength steel. Typical applications are details for mobile cranes and vehicles for heavy-duty transports; examples are given in **Figures 1** and **2** [1].

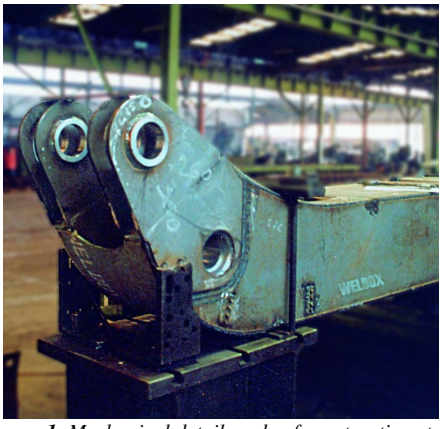

***Figure 1**. Mechanical detail made of construction steel.*

***Figure 2**. Vehicle for heavy-duty transports.*

The following requirements are generally made on heavy plate. They must

- possess the specified dimensions within narrow tolerances and with good flatness. Order thicknesses may range from 4 to 130 mm and widths from round 1 to 3.4 m may be selected;
- possess the yield strength and tensile strength figures by the designers, yield strength from 350 MPa to around 1300 MPa can be specified;
- possess the toughness required by designers even at low temperatures;
- possess good deformability and weldability [2].

The properties are in some cases contradictory. Thin gauges of these materials can allow the same load as thick gauges of mild steel [1]. The state of the art heavy plates nowadays, are quenched and tempered 4-6 mm thick material in widths of about 2000-3300 mm.

The production steel in Oxelösund is based on ore. See **Figure 3** for an overview.

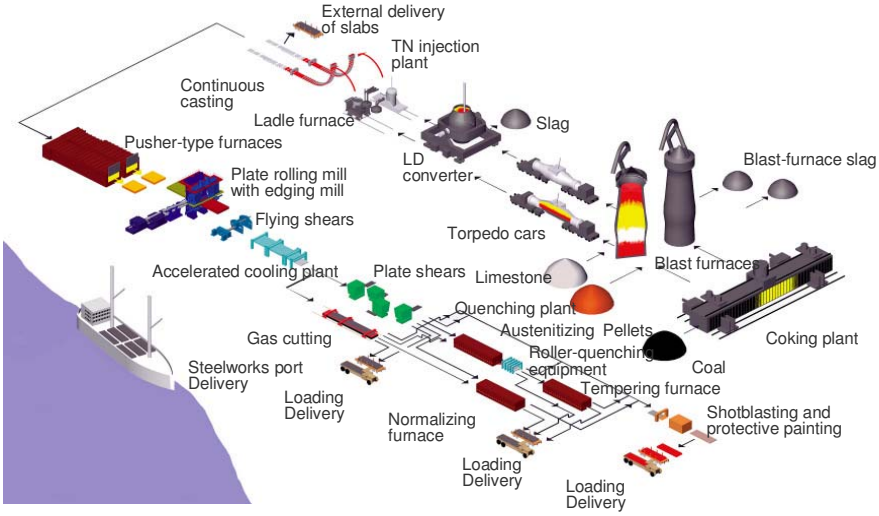

Figure 3. *The flowchart of heavy plate production in Oxelösund.*

All the material is reheated before rolling up to 1160-1245 ℃. The weight of the plates is between 1.6 and 13.3 tons. The slab thickness is normally 220 mm, but also 290 and 140 mm exist. The rolling is carried out in a modern and very powerful four-high mill from 1997, shown in **Figure 4**. See also Paper B for more details. The strain rate varies between 0.5/s up to 50/s. The finishing rolling temperature varies in the range of 650-1160 ℃. The plate is normally quenched, tempered, leveled, formatted and painted after rolling. The products are delivered world wide from the steel port, by train or by lorry. The rolled tonnage totaled 793 000 tons during 2005.

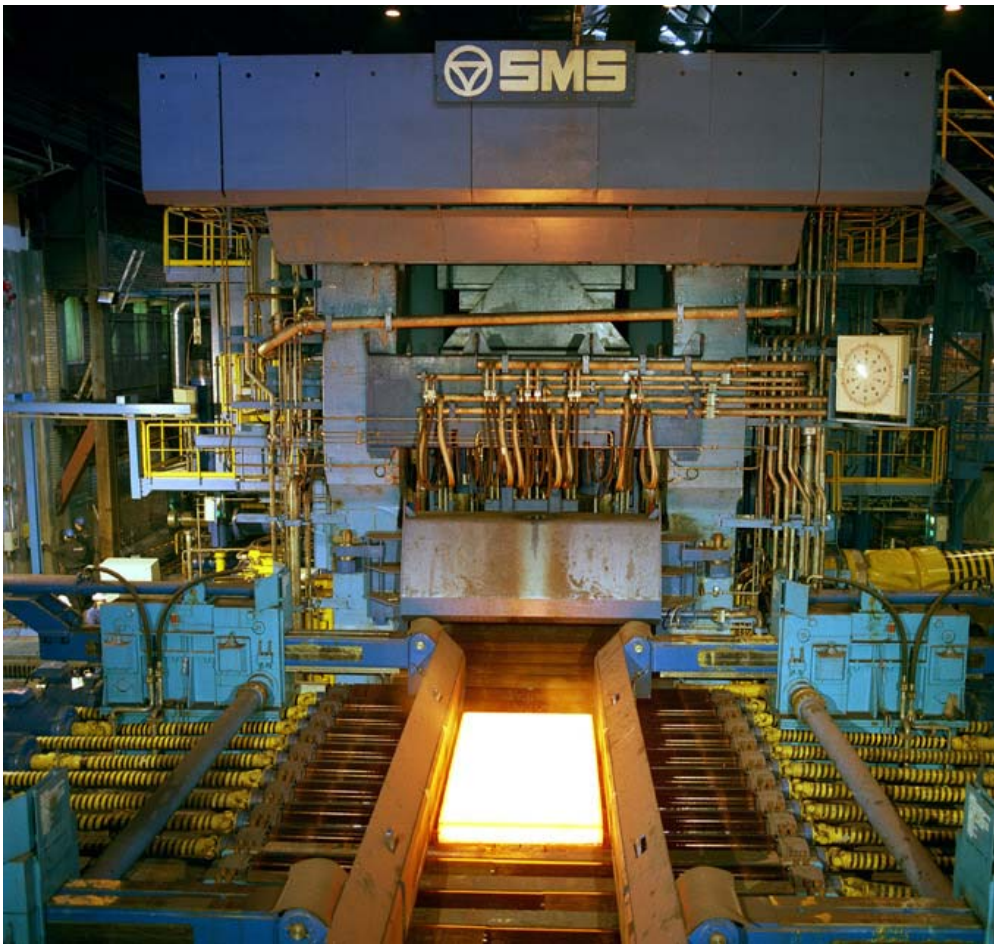

Figure 4. *Rolling in the heavy plate mill in Oxelösund.*

2.1 The rolling process

The traditional equipment for rolling of heavy plate is the four-high mill. This mill has four rolls, two weaker work rolls and two sturdier back-up rolls. The work rolls get in touch with rolled material and reduce its thickness. The back-up rolls counteract the deflection of the work rolls and increase the stiffness in the mill. The rolling force is defined as the force derived from the rolled material that acts on work rolls [3]. Because of the contact between the back-up rolls and work rolls is the rolling force in practice taken up by the back-up rolls. Besides, the work roll bending force acting on the roll necks and the dead weight of the rolls are also included to the load on the back-up rolls, see **Figure 5**.

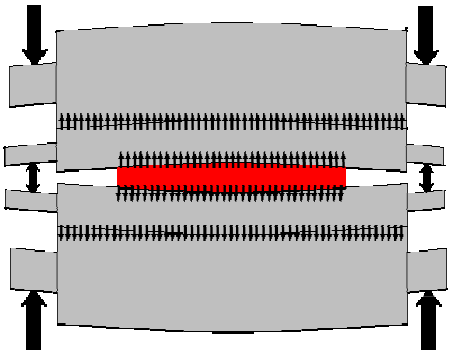

***Figure 5**. Principal sketch of a four-high mill with forces from the plate, the work roll bending and back-up roll bearings exposed.*

Drawing of the roll gap transverse to the rolling direction makes it possible to define the work roll radius r, the contact length l_{d-1}, the entry thickness h_0 and the exit thickness h_1 see **Figure 6**.

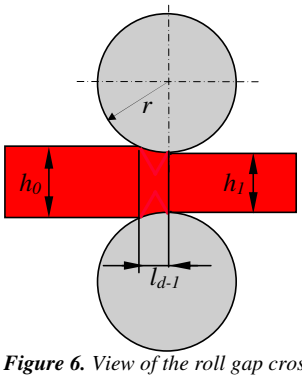

***Figure 6.** View of the roll gap cross the rolling direction.*

Usually, it is assumed that the cross section is constant along the plate width. Sometimes, this assumption is accurate enough. Otherwise, the variations of the roll deflection must be considered. Modeling of the plate crown, flatness and roll wear are examples of cases where the varying roll radius must be accounted for and therefore demand a three-dimensional model.

Accurate on-line models for the pass schedule are needed in a modern rolling plant for a wide production mix of steel grades, target gauges and widths. Prediction of process parameters with respect to reduction, rolling force and flatness is necessary to obtain a good result. The thickness, flatness and stability are important quality factors direct influenced by the rolling process parameters. In addition, thin gauges are prone to instability and breakdown due to buckling in the final passes if the rolling parameters are not chosen carefully. A breakdown in the mill due to buckling results in low productivity because of the cleaning and repair works afterwards. **Figure 7** shows a plate after buckling and breakdown.

Figure 7. *A thin plate after buckling and breakdown.*

The productivity in the mill is also strongly affected by the choice of thermomechanical pass schedules, due to the long cooling pause needed to obtain a refined microstructure. Proper models for thermomechanical rolling are desirable. Also the time for changing work rolls due to wear decreases the productivity and is expensive.

2.2 Deformation in the rolling process

The forces in the mill cause elastic deformation of its components. The rolls are bent during the rolling. If nothing was done to reduce this, then the thickness of the plate will vary and the plate edges would be more elongated in the rolling direction, see **Figure 8**. If the middle of the plate becomes more elongated than the edges, the result will be center buckles, **Figure 9**.

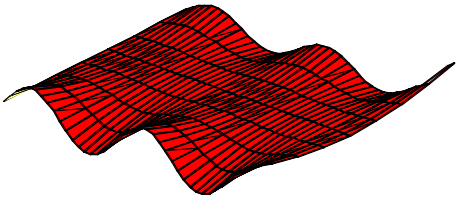

Figure 8. *A plate with more elongated edges than the middle. The elongation results in wavy edges.*

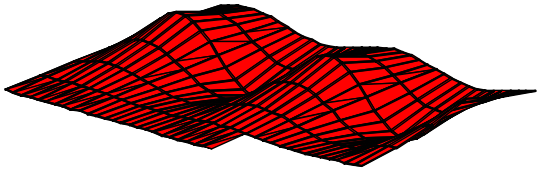

Figure 9. *A plate with center buckles. The middle is more elongated than the edges.*

The term crown denotes a variation in the roll radius used to improve the flatness of the plate. The crown is defined as the difference between the centre thickness and the thickness close to the edge. **Figures 10** and **11** demonstrate the two main principles for the plate crown, positive and negative, respectively.

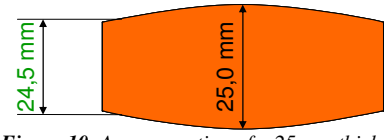

Figure 10. *A cross section of a 25 mm thick plate. The crown is 0.5 mm.*

Figure 11. *A principal sketch over a cross section with negative crown.*

There are also other methods in the mill for controlling the thickness of the plate. The most effective in the mill in Oxelösund is the CVC-system, see **Figure 11**, **12** and **13**. The CVC-technique is based on variable work roll diameters. Shifting of the roll position in axial direction admits influence of the roll gap and the plate crown, as well. The CVC-position is critical for the flatness result and has to be correct prepared before every pass, since it is not possible to change CVC-position during operation.

Figure 12. *Positive CVC-shifting gives a negative plate crown.*

Figure 13. *Neutral CVC-shifting gives a neutral plate crown.*

Figure 14. *Negative CVC-shifting gives a negative plate crown.*

The work roll bending system is dynamic and subjects the work roll necks for varying bending forces. **Figure 15** contains a sketch over the work roll bending. The effect from the work roll bending is much less than the effect from the CVC. The work rolls are also subjected to thermal loading during hot rolling. The roll temperature and thereby the thermal expansion is non-uniform due to cooling and rolled plate widths. **Figure 16** illustrates the thermal expansion on the work rolls. Wear is caused by the thermomechanical contacts between the plate, work rolls, and back-up rolls. The plate edges are the major cause of wear during a pass. **Figure 17** illustrates the phenomenon. Schedule-free rolling means that production mix is not sorted with respect to the plate widths. The CVC-shifting helps to spread out the wear along the barrel and is therefore a useful tool for schedule-free rolling. This procedure requires a high accuracy of model for prediction of the work roll wear contour. The result of flatness and stability will be affected of the sum of all the factors mentioned above. Moreover, the productivity can also be influenced if the wear contour model overestimates the amount of wear and causing a too early change of work roll.

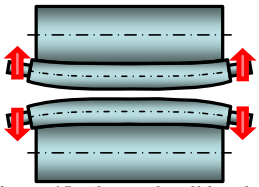

Figure 15. *The work roll bending system.*

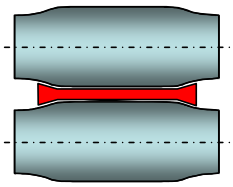

Figure 16. *The thermal expansion of the work rolls.*

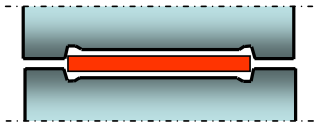

Figure 17. *The worn work rolls.*

2.3 The overall strategy in the mill

The rolling is the crucial link in an expensive and complicated manufacturing process. The utilizing of the rolling mill in an effective way with retained high product quality is important. Planning and controlling the process can be done in several ways, the production mix has an influence for the choice of method. A mix dominated of a uniform product, with respect to chemical composition and geometric dimensions can be rolled with a fixed pass schedule, particularly for thick final gauges. Then the process can be planned with focus on this product. The drawback is that the plates that differ from this product can cause severe quality and productivity problems.

The solution of this problem is to employ an on-line model to set up separate pass schedules for every plate. In a plate mill now days, this solution is the only possible, since the customers asks for tailor made heavy plates, with respect to steel grades, widths, lengths and gauges.

3 Modeling to improve the rolling process

Models of the rolling process can be developed with respect to different scopes and application contexts. The different context they might be used in are:

- Research level. The focus is on high accuracy, while the time for the simulation is not critical. Examples of tools in this category are the Finite Element Method (FEM), but also other simulation techniques like the Finite Difference Method (FDM), the slab element method or the upper bound analysis. Also methods for simulation of the microstructure evolution, the MicDel-software should be mentioned [4]. The benefit is the high resolution of the state in the roll gap and possibility to simulate different kind of contact conditions. The drawbacks is that it can be very time consuming to created the models and/or perform the simulations. Two dimensional simulations are considerably simpler and faster. However, many research questions, like prediction of flatness and roll wear, require three dimensional models. One problem is how to account for the elastic deformation of the rolls. On the whole, FE-analysis is proper for demanding research questions when two dimensions are suitable and a few number of geometries are enough to answer the asked for question.
- Engineering level. The engineering models are determined by means of fitting model equations and parameters with experimental data. Commonly used for on-line models in the process computer in the mill. The demands on the on-line models are safe and very fast answers, and acceptable accuracy. Good engineering models fulfill these, and make it possible to handle three dimensional effects and the whole range of existing combinations of geometries and material properties. The drawback is often limited resolution of the current state in the roll gap and limited accuracy in general. They are heavily dependent on appropriate calibration procedures for their parameters and thereby not usable for new procedures and materials.

3.1 Combination of methods for research and engineering levels

The goal with the current work is to develop models useful for on-line control of the rolling process. This can be done by the approach shown in **Figure 18**. The use of information from research level models has not been used yet in the work in this thesis. The basis is adaptation of models taken from the literature combined with measurements from the rolling mill, process data, and laboratory testing.

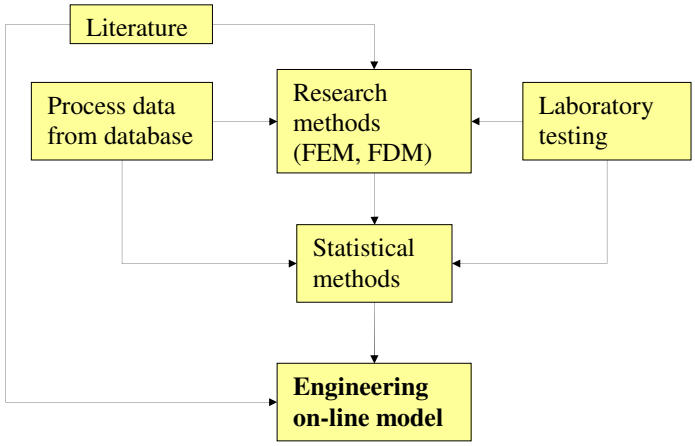

Figure 18. *Flow chart for development of engineering on-line models.*

A modern steel plant houses process data bases. These databases are continuously updated. The use of multivariate technology turns the data into vital information. Different factors in the models must be calibrated by comparison with measurements before they are useful in optimisation of a process or procedure. The more physically based the models have, the less is the need to calibrate them with process parameters. They are instead based on more fundamental measurements of material and friction properties. Especially, the latter can be difficult to obtain for rolling conditions. Another disadvantage is that they may require a large computational effort. Although less elegant, statistical models can be used efficiently and be very accurate in a limited interval, which depends on the range of conditions used to calibrate them [5].

3.2 Design of experiments

The design of experiments is a technique to organize the experimental work into a minimum of work input and a maximal information output [5]. The strategy is to vary all factors simultaneously in a planned set of experiments. The importance of each factor can be estimated separately, and the interaction between them if any.
The basic idea is to devise a small set of experiments, in which all pertinent factors are varied systematically. This set usually does not include more than ten to twenty experiments. The subsequent analysis of the resulting experimental data will identify the optimal conditions, the factors that most influence the results and those that do not, the presence of interactions and synergisms, and so on. The most important aspect of design of experiments is that they provide a strict mathematical framework for changing all pertinent factors simultaneously, and achieve this in a small number of experimental runs. Each planned experiment gives results i.e. values response variables. Thereafter, these data are analyzed by means of multiple regression, or generalizations thereof such as Partial Least Squares projection to latent structures (PLS) or Multiple Linear Regression (MLR). This gives a model relating the factors to the results, showing which factors are important, and how they combine in influencing the results. The model is then used to make predictions, e.g. how to set the factors to achieve desired results [5].

4 Thermomechanical rolling

Due to the fact that steel is softer the higher the temperature, it is generally rolled at temperatures high in the austenitic region. However, the mechanical properties of the steel are generally improved by a relatively low temperature treatment such as normalizing which refines the structure. The demands for high yield strength and other strengths in large-diameter pipelines, combined with high toughness at low temperatures and good weldability, have resulted in thermomechanical rolling [2]. In the beginning of the 1960´s, some European steel producers were controlling the rolling process to deliberately finish rolling the steel at temperatures lower than usual in order to refine the micro structure and improve properties. Thus, removing the need for a further treatment stage. There is a potential for energy saving, since the reheat- quenching-tempering process is not needed. The principal cause of the improvement of the mechanical properties is the general refinement of the micro structure resulting from the refinement of the austenite during hot working [8]. The procedure is known under different names, controlled rolling, recrystallization controlled rolling or ThermoMechanical (TM) rolling.

4.1 Mechanical properties

High-strength structural heavy plate in gauges up to 40 mm with yield strength up to 420-500 MPa can be produced with TM-rolling today. An ACcelerated water Cooling (ACC) direct after rolling can be performed on thicker gauges to reach the yield levels [2]. Grain refinement is one of few methods available for strengthening. This is often expressed by the Petch-Hall relation [6]. TM-rolled plates have a very attractive combination of high strength and ductility due to the fine microstructure [8].

4.2 Grain refinement

The major purpose of TM-rolling is to refine the ferrite grain size of the steel. In fact, it appears that a ferrite grain size of approximately 1 µm is a practical lower limit in low alloy steels. In commercial, ferrite grain sizes of ~5 µm may be obtained in TM-rolled thin microalloyed plates [7]. TM-rolling involves an extra demand on the rolling process. The pass schedule must be proper to ensure right material properties after rolling. The grain refinement is obtained by substantial thickness reductions and decreased rolling temperature. In order to optimise the rolling process it is necessary to understand the relation between the structure and the properties and how the micro structure is affected by hot deformation [8]. The active parameters affecting the microstructure are temperature, reduction, time, chemical composition, strain rate and the microstructure itself. In principal is there a relation; the lower the finishing rolling temperature the finer the ferrite grain size. In order to reduce the finishing rolling temperature, the TM-process includes a long delay time during the pass schedule. The long delay time before the final passes triggers recrystallization and thereby promotes a final structure of fine grains. The chemical composition has an important effect on the grain refinement, particular Nb, which slows down the recrystallization and the grain growth of the austenite [9]. **Figure 3** in Paper A shows the development the austenite grain size during the pass schedule. The austenite grain refinement is particular obvious during the first passes. However, commercial TM-pass schedules may be completed while the steel is undergoing transformation from $\gamma \rightarrow \alpha$ so that the ferrite becomes deformed. It is difficult to refine the grain size in the ferrite region due to the ease of recovery of ferrite compared with austenite, resulting in a tendency for sub grains to form within elongated ferrite grains. Therefore, the target thickness should be reached before the transformation starts [6].

4.3 Strategies for successful TM-rolling

The TM-material can be produced in any single-stand plate mill. The material undergoes reheating at normal temperature, commonly at 1160-1170℃. Then the roughing stage follows at normal rolling speed down until the holding time. This pause is inserted in order to allow the plate to cool in order to trigger the recrystallisation. During the holding time, the plate is cooled in air on the roller table. The holding thickness at this instance varies, but a rule of thumb is about 3 times the final gauge. The drawback with this pause is that it affects the productivity negatively and therefore it should be as short as possible. The finishing rolling follows after the pause. A common method to generate pass schedules for TM rolling is to limit the temperature in the last pass and specify a holding thickness. Some ironworks with a high production rate of TM-plate of one format, evaluates different pass schedules with respect to productivity and material properties after rolling [6] in order to find a suitable schedule. A further approach towards optimising productivity by minimizing holding delays is to deliberately reduce the reheat temperature. The temperature in the end of the roughing then becomes closer to that required for entry into the finishing sequence. However, there is a risk for hydrogen defects and a more complicated controlling of the reheat furnace is required. The strategy proposed in Paper A is based on prediction of the grain size instead of more commonly focus on temperature only. The developed code for the microstructure behavior accounts for recrystallization, austenite grain size, contents of niobium and titanium and precipitation. The simulated austenite grain sizes show good agreement, compared with results from full-scale experiments.

5 Wear in the rolling process

The work rolls in the mill are subjected to periodic loading that is accompanied with abrasion by scale and fluctuations in temperature [10]. A work roll wear contour is shown in **Figure 19**. The rolled material was a mix of different plate widths, steel grades, lengths and gauges. The wear contour is so to say a mirror of the produced material. Thanks to the sampling and storage of process data it is possible to recalculate rolling of the plates and tune the model for the wear contour. The “negative” wear at -1815 mm from the middle of the work roll barrel, is due to errors in the measurements.

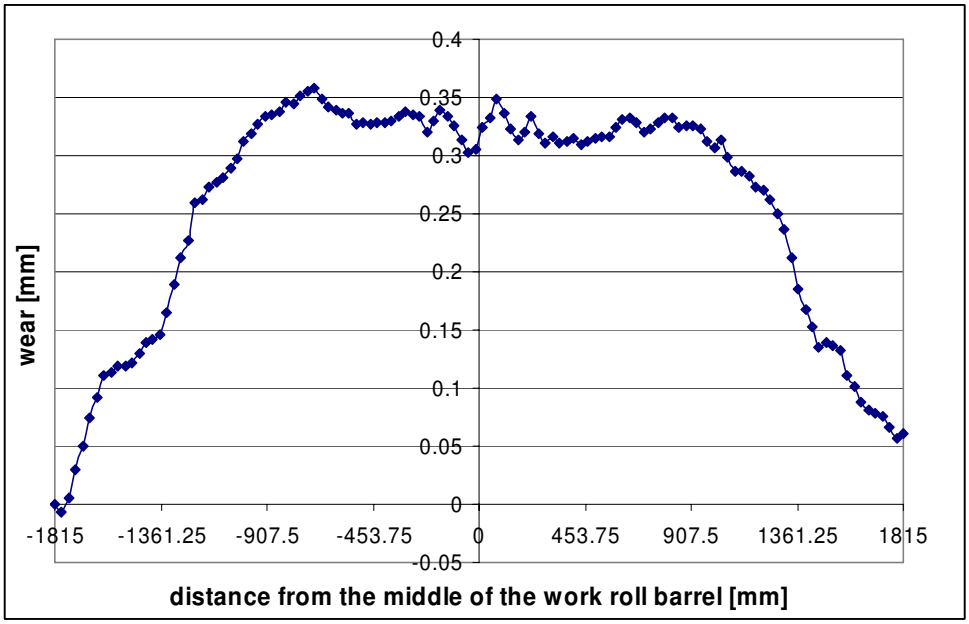

Figure 19. *The wear contour of a work roll after rolling of a campaign.*

5.1 Different strategies to model the wear contour

There are a number of methods that can be used for the calculation of the work roll wear contour:

1. Develop a model for prediction of the absolute local roll wear C_m [mm] in the middle of the roll barrel caused by the plate, neglect the wear caused by the back-up roll and assume that the local wear at the edge C_e [mm] of the plate, is proportional to C_m:

$$C_e = kC_m \quad \text{.....(1)}$$

Nakanishi [11] found that when the roll wear geometry at the strip edges is defined by a= 10 mm and b= 50 mm, that the wear increase coefficient k =1.3

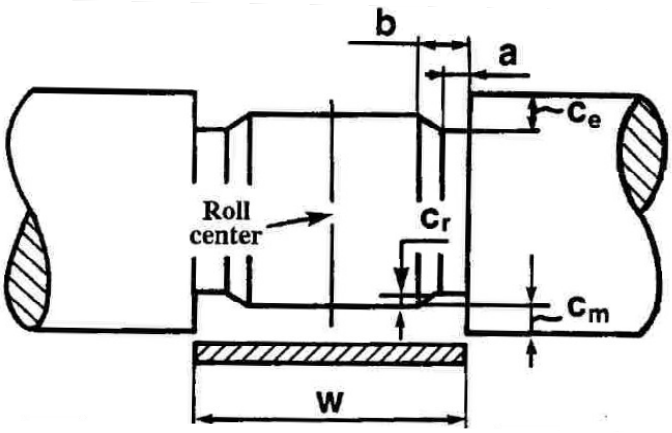

Figure 20. *Modeling of the absolute local roll wear at the middle C_m in the middle of the roll barrel and edge C_e. Adapted from Nakanishi [11].*

The benefit with equation (1) is the simplicity and swiftness in the use of it. The drawbacks are poor accuracy due to that only the wear caused by the plate is taken into consideration and that the value of k is not fixed for every passes.

2. Build up a non-linear wear prediction model for the roll barrel based on the combination of theoretical study and actual measurements. Lin et al [12] proposed following wear model for calculation of the work roll wear $C(x)$ in an arbitrary position x along the barrel:

$$C(x) = k_{w0} \cdot \left(Q_1(x)\right)^{k_{w1}} \cdot \frac{L_{Plate} \cdot l_{d-1}}{r}(1 + k_{w2} f_{wx}) \quad \ldots\ldots\ldots\ldots\ldots\ldots\ldots\ldots\ldots\ldots(2)$$

where k_{w0}, k_{w1}, k_{w2} are empirical coefficients depending on the roll material, lubrication, L_{plate} is the exit plate length, $Q_1(x)$ is the rolling pressure it current x-position and f_{wx} is a function of irregular roll wear on axial direction:

$$f_{wx} = \begin{cases} 0 & x < -1 \ \ or \ \ x > 1 \\ a_0 + a_2(x)^2 + a_4(x)^4 & -1 \le x \le 1 \end{cases} \quad \ldots\ldots\ldots\ldots\ldots\ldots\ldots\ldots\ldots\ldots(3)$$

where a_0, a_2, a_4 are irregular wear coefficients within range of plate width W. See **Figure 21** for further details.

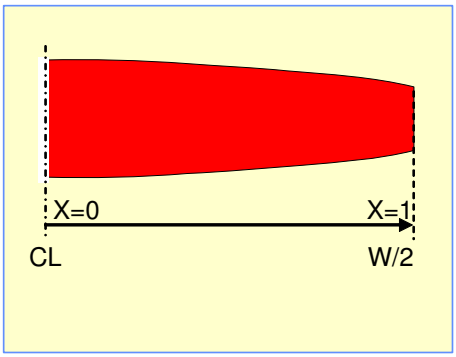

Figure 21. *Symmetric cross section of a plate from the centre line CL to the edge W/2. Demonstration of x.*

The value of x=0 in the center line CL of the plate and x=1 on the edge of the plate, independent of the plate width. The benefit with the approach is a more flexible description of the wear contour than equation (1) due to the circumstances. The drawbacks are that still only the wear caused by the plate is considered and a demanding optimisation procedure of the ingoing coefficients in equation (2) and (3). Lin et al [12] used Simulation Annealing Theory and Application (SAA) for fitting and optimisation to receive a proper result.

3. Develop a neural network for calculation of the wear contour. The principal is that the neural network is fed with process parameters from the rolling process and that these parameters are treated mathematically. The output is the wear contour [13]. The advantage is that the network can find and identify patterns. Artificial neural networks learn from studying examples and thus the user do not have to describe the actual pattern with a mathematical formula. They are also useful when demanding calculations are needed to obtain the solution and the relations between input and output are known but not the equations between them. The disadvantage with neural networks is on the whole the period for training. It may take too long time to obtain all combinations and even longer time to train the network. There is simultaneously a risk for overtraining. That makes it hard to interpret and understand the underlying calculations of a solution. If poor accuracy occurs, the reason is hard to trace and take care of.

4. Use a method based on simulations with FEM or FDM of every pass in combination with a wear model. CROWN426 is a computer program for simulation of profile and flatness during flat rolling based on FDM. CROWN426 takes elastic deformation of the mill, thermal expansion, and work roll wear into account in the simulations [14]. CROWN426 uses the following expression for $C(x)$:

$$C(x) = k_w L_{plate} Q_1(x) \frac{\sqrt{1 + \dfrac{16 Q_1(x) \dfrac{(1-\upsilon^2)}{\pi E}}{h_0 - h_1}}}{2\pi r} \quad \text{.....(4)}$$

where k_w is a wear coefficient, υ is the Poisson's ratio[--], E is the modulus of elasticity for the roll [MPa]. The idea of the use of the variable rolling pressure $Q_1(x)$ is to handle both the overall and local wear. The drawback of the method is a time demanding simulation (~30 s. per pass) with CROWN426 to obtain $Q_1(x)$ and the contribution to the wear from the back-up

roll is not estimated. Simulations with commercial FEM-programs are even more time consuming and are in practical not realistic on-line control of the rolling process.

5. Develop a method that combines the results from a handful of well chosen FDM-simulations with statistical methods to receive explicit expressions for the wear on the work roll barrel caused by the plate and the back-up roll. The benefit is that a high number of variants with respect to rolling conditions can be taken into account and that the information from the simulations is well treated. The optimisation procedure to measured data can also be performed in a relatively competitive way. Adjustments can also be done fairly simple. The drawbacks are that a number of well-planned FDM- or FEM-simulations are required, the following PLS- or MLR-analysis and fitting and testing of the model to measured data, as well. This approach was used in Paper 2.

6 Summary of appended papers

6.1 Paper A

In this paper, a strategy for controlling TM-rolling is proposed. Simulation of the final microstructure after rolling and accelerated cooling is the basis for determining roll pass schedule. The rolling is modeled with different lengths on the long interpass time, which is important for the final microstructure. The microstructure model treats accumulated strain, austenite grain size, static and metadynamic recrystallization, grain growth, precipitation of Nb(C, N) and ferrite grain size after transformation from austenite. The conclusions show that the influence from the long interpass time affects both the ferrite grain size as well as the productivity. If the long interpass time is too short, there is not any greater use of it. On the other hand, a too long delay time does not improve the ferrite grain size but worsen the productivity.

6.2 Paper B

The paper presents a model of the wear contour along the barrel of the work rolls. The background to the model was found in the literature. The wear contributions from the rolled plates and the back-up rolls were taken into account. The amount of wear in any point was considered to be proportional to the contact pressure in the point and the number of roll passes. Statistical models for the variation of the specific rolling force along the work roll barrel were determined. Design of experiments was used to create a number of passes for simulation with CROWN426. The statistic models were built up on results from simulations, considering that the load distribution can be expressed with polynomials. The wear contour model was thereafter calibrated against a number of measurements from the rolling grinder. The model was calibrated and showed good agreement with the measurements.

7 Discussions

Two aspects of modeling and controlling the rolling process have been studied.
The first one is the choice of rolling pass parameters in Paper A. The roll passes are determined by using models for the final grain size of the plate instead of the current approach where only the temperature is monitored. The microstructure evolution is only determined as an average value over the cross section. A better approximation should be if the cross section was discretized into a number of segments. However, this improvement will require accurate models for the variation of strain and strain rate in the thickness direction.
The second aspect is the modeling of roll wear in Paper B. The simulations of the specific rolling force were carried out on the simplifying assumptions that the CVC-grinding profile, the CVC-position, the thermal crown, wear and work roll bending do not affect the specific rolling force between the work roll and back-up roll. However, the fundamental parameters rolling force, work roll radius and back-up roll radius were all included in the current model, even the plate width since it was identified as a significant parameter. The wear coefficients are strongly dependent of the properties of the work roll material and the scale on the hot plates. Every work roll can probably be considered as an individual due to certain deviation in the manufacturing process of the rolls. The mechanical properties of the scale vary very much dependent on the temperature and presumably there is also an effect from the chemical analysis of the plate. As a result, the wear regime in the roll gap can vary as well. This phenomenon appears as the most significant part for further investigations due to the fact that the most of the total wear is caused in the contact of the plate and the work roll.

8 References

[1] L. Bergqvist: ”Konstruera med EHS- och AR-plåt”, SSAB Oxelösund AB, Oxelösund Sweden, (1987).

[2] B. Ahlblom: Proc. of Stålindustrins värmnings-bearbetnings och materialpaket 1999-2003, Jernkontoret, rapport D 797, projekt 31042, (2003), pp. 4-5.

[3] T. Nilsson, P. Huml, U. Ståhlberg, T. Engelbert, S. Essle, K. Larsson, U. Öhman: ”Massivomformning, Verkstadstekniska processer, Tribologi, Formelsamling”, Institution for metal working, Royal Institute of Technology, Stockholm (1986).

[4] P. Hansson: PhD Thesis, Institution for industrial production, Royal Institute of Technology, Stockholm (2004).

[5] Umetrics AB: MODDE 7.0, “Users Guide and Tutorial”, Umetrics, Sweden, (2003).

[6] R. K. Gibbs, B. A. Parker, P. D. Hodgson: “The prediction of ferrite grain size in niobium microalloyed controlled rolled steels”, The Minerals, Metals & Materials Society, Recrystallization’90, ed. By T. Chandra, (1993), pp. 173-177.

[7] Y. Z. Zheng, A. J. DeArdo, R. M. Fix, G. Fitzsimons: Proc. of HSLA Steels, Technology and Applications, Philadelphia, (1983), pp. 85-94.

[8] W. B. Morrison, J. A. Chapman: “British Steel Corporation, GS/PROD/MISC/107/75/C”, (1975), pp.1-2.

[9] A. Köthe, J. Richter, A. Güth, L. Kaun, G. Backmann, M. Schaper, U. Gutteck: „Recrystallization-controlled rolling of C-Si-Mn-V-N steel“, Institut für Festkörper- und Werkstofforschung Dresden, Germany, (1989).

[10] C. L. Robinson and F. J. Westlake:” Roll Lubrications in Hot Strip Mills”,Conf. Proc. of the First European Tribology Congress, London, Sept. 25-27, (1973), pp. 389-398.

[11] T. Nakanishi, T. Sugiyama, Y. Lida: “Application of Work Roll Shift Mill HCW Mill to Hot Strip and Plate Rolling”, Hitachi Review, vol. 34, no. 4, (1985), pp. 153-160.

[12] S. Lin, L. L. Bingman, Z. Xiang: “The applications of Simulated Annealing Algorithm to Improve Wear Models in Plate Mills“, Conf. Proc., 44th MWSP, vol. XL, (2002), pp. 593-603.

[13] R. Turk, P. Fajfar, R. Robic, I. Perus:”Prediction of hot strip mill roll wear”, Metalurgija (Yugoslavia). vol. 41, no. 1, Jan.-Mar. (2002), pp. 47-51.

[14] J. Levén: “User’s Manual CROWN426”, MEFOS Metal Working Research Plant Sweden, (2004).

A

An investigation of different strategies for thermo-mechanical rolling of structural steel heavy plates

Mikael JONSSON
SSAB Oxelösund Ltd. GVT SE-613 80 Oxelösund, Sweden.
E-mail: mikael.jonsson@ssabox.com

Abstract
A software has been developed to determine optimal rolling passes in thermo-mechanical (TM) rolling in order to obtain a fine microstructure. It includes models of the effect of strain, precipitates, static and dynamic recrystallization and austenite grain size on the final grain size. It was also used to study the effect of different long interpass times during thermo- mechanical rolling of heavy plates. The predicted grain sizes for four different cases were compared with experimental results.
KEY WORDS: plate, thermo-mechanical rolling, recrystallization, rolling strategy, grain size, precipitation, pass schedule generation.

1 Introduction

High-strength structural steel plates with yield strength up to 500 MPa can be produced with thermo-mechanical (TM) rolling and accelerated cooling immediately after the rolling[1)] giving a fine grained material with good ductility and a high strength[2)]. There is a great potential for energy saving by optimization of the TM process, since no reheat quenching tempering process is needed. Furthermore, the weldability of the plate becomes very good as the chemical composition of the plate can be kept at a low level[1)]. The grain refinement is obtained by substantial thickness reductions at decreased rolling temperature. The TM process includes a long interpass time during the pass schedule[3)]. The long interpass time before the final passes triggers recrystallization and thereby promotes a final structure of fine grains.
The aim of this work was to develop a pass schedule planning software on basis of the microstructural evolution in the steel during TM rolling. Knowledge of the rolling parameters and process limitations associated with the TM rolling makes it possible to design proper rolling schedules for obtaining a good end product and acceptable productivity.
A common method to generate pass schedules for TM rolling is to limit the temperature in the last pass. The strategy to control the rolling process proposed in this paper is based on predicted grain size instead of temperature only. The developed code for the microstructure behavior accounts for recrystallization, austenite grain size, contents of niobium and titanium and precipitation. The simulated austenite grain sizes show good agreement, compared to results from full-scale experiments.

2 Method

2.1.1 Overall logic in the pass schedule generator

A Visual Basic program was developed for simulation of microstructure during a pass schedule. The program simulates a complete pass schedule for rolling of a heavy plate in the four-high mill at SSAB Oxelösund. The program determines the reduction in each pass and also specifies the long interpass time in order to obtain a fine final microstructure. The required CPU-time is around 5 minutes for simulating a complete TM pass schedule.

The overall logic is shown in Figure 1**.** The program attempts to reduce the thickness by 50% in each pass without exceeding available force and torque with a profile within the tolerances. If this is not achieved, then a smaller reduction is tried. The generator strives for reaching the target thickness h_{tar}. The roll force model gives roll force and torque. CROWN426 is a program package for simulating thickness profile and flatness in flat rolling. The elastic deformation of rolls and the deformation of the rolled material are calculated for both hot and cold rolling mills with 2-6 rolls. Force distributions between rolls and work roll profile are calculated. The assumed reduction together with the prediction of profile by CROWN 426 gives the accumulated plastic strain. The latter program is only used when the thickness is below 80 mm. STEELTEMP® 2D is a program for temperature and heat-transfer analysis during casting, cooling, stripping, heating, rolling and forging. Temperatures and densities of heat flow rate are calculated in a cross section of the steel. The temperature evolution during and between the roll passes is computed by STEELTEMP® in this investigation. The lengths of the interpass times are in the range of 5-15 [s] and depend on the practical handling of the plates. Thus they depend on the length of the plate, and are known from common rolling schedules and tabulated in the program. The plate is rotated between the initial passes but not after the 4th pass and it is cooling slowly also during these initial passes as it is quite thick. Therefore the long interpass time is not placed until after the fourth pass. Its length is never allowed to exceed 10 minutes for productivity reasons. The scheduler determines appropriate length of the long interpass time. The scheduler currently chooses only between one, five or ten minutes. It is possible to find the exact optimum that minimizes the final grain size by optimization. The limitation currently imposed by choosing between a given set of times is made in order to limit the calculation time. The microstructure model uses the temperature and deformation to predict the microstructure. The roll-force and microstructure model are described below whereas STEELTEMP is described in Reference 4 and CROWN 426 in Reference 5. Subscripting is used for some of the variables in the following description of the theory implemented in the roll pass scheduler and summarized in Figure 1. Subscript 0, $[\ ]_0$, means entry value to a pass and subscript 1, $[\ ]_1$, means exit value after the pass. Thus the exit values become entry values after each roll pass is analysed.

2.2 Model for rolling force

The roll force F [N] model used by the roll pass generator is

$$F = 1.15\sigma_y L_d b k_{Pawelski} = 1.15\sigma_y L_d \left(\frac{b_0 + b_1}{2} \right) k_{Aspect\,ratio} \qquad (1)$$

where 1.15 is a correction factor due to plane strain assumption, L_d [mm] is the contact length between the work roll and the material including the effect of roll flattening, b [mm] is the mean width of the entry width b_0 and the exit width b_1 and $k_{Aspect\,ratio}$ [--] is a correction factor for friction and inhomogeneous deformation[6].

The spread is calculated with the method derived by Beese[8] for commercial rolling of low carbon steel slabs

$$b_1 = b_0 \left(\frac{h_0}{h_1} \right)^{0.6 \frac{h_0}{b_0} e^{-0.32 \frac{h_0}{L_d}}} \qquad (2)$$

h_0 and h_1 is the entry and exit thicknesses [mm], respectively.

The flow stress σ_y [MPa] is determined with the modified Misaka equation[7]

$$\sigma_y = g \cdot e^{(0.126-1.75C+0.594C^2+\frac{2851+2968C-1120C^2}{T})} (\frac{\varepsilon_0^p + \varepsilon_1^p}{2})^{0.21} (\dot{\varepsilon}_1^p)^{0.13} f \qquad (3)$$

where g is the constant of gravity 9.8 [N/kg] needed to convert the units from [kg/mm^2] to [MPa], C is the carbon content in weight percentage [%], ε_0^p [--] is the entry plastic strain in the pass, ε_1^p is the exit strain from the roll gap:

$$\varepsilon_1^p = \ln(\frac{h_0}{h_1}) + \varepsilon_0^p \qquad (4)$$

$\dot{\varepsilon}_1^p$ [1/s] is its strain rate, T [K] is the absolute temperature. The factor f [--] is a correction function of the contents of alloying elements niobium Nb, manganese Mn, and titanium Ti, all in weight percentage [%]. This value is computed as

$$f = 1.15 \cdot (0.768 + 0.51Nb + 0.137Mn + 4.217Ti) \qquad (5)$$

The factor 1.15 in Eq. (5) is based on statistics from measurements of the rolling force in Oxelösund. The reason is that the used steel grades also contain other alloying elements such as chrome, vanadium, molybdenum and nickel. The exit plastic strain computed by Eq. (4) may be modified, as described later, in case recrystallization occurs.

2.3 Modeling of the microstructure

The grain size evolution is calculated by a microstructure model. The complete flow chart for the microstructure model is shown in Figure 2.
The effective plastic strain and plastic strain rate together with temperature are driving the changes in grain size. The model is accounting for grain growth as well as recrystallization.
There are many reports giving grain sizes for micro-alloyed steels after reheating. This grain size is the initial value for the roll pass scheduler. Köthe[3)] reported that the grain size is below 100 µm at 1250 °C. Zheng and co-workers[14)] stated that 200 µm is a good approximation for a V-Ti steel after 1 hour reheating at 1170°C. Hong and Park[20)] used 200 µm in their investigation. The initial grain size before the rolling is taken as 200 µm in the current work Furthermore, it is assumed that there exists no precipitation of Nb(C,N) or accumulated plastic strain in the beginning.
Recrystallization can be prevented by strain induced precipitation. Thus the program starts with computing the amount of precipitation. If too much precipitation has occurred, then there will be no recrystallisation else it is determined whether the recrystallization is metadynamic (MDRX) or static (SRX). Thereafter the effect of recrystallization on the accumulated plastic strain and grain size is computed. Grain growth is only computed after recrystallization is complete. Finally, it is predicted what the final microstructure, ferrite grain size, would become if the plate is cooled to room temperature in the current state. The details of the model are explained below.

2.3.1 Precipitation model

Significant strain induced precipitation effectively stops SRX that might occur during the short time for the reduction during the rolling[25)]. Abad *et al.*[11)] established that the precipitation needed to reach 5% completion in order to be effective to prevent SRX. Hence, it is assumed that if 5% precipitation is reached then no SRX occurs.

The Dutta and Sellars model[25] describes the strain-induced precipitation from supersaturated austenite, under isothermal conditions. Since the model was derived under isothermal conditions, the additivity rule[11] was employed to enable its application during cooling. The criterion for 5% precipitation is written as

$$\sum_{T_0}^{T_1} \frac{\Delta t}{t_{0.05m}(T_j)} = 1 \qquad (6)$$

where Δt is the time increment the cooling curve is divided into. It is taken as 0.1 s. Furthermore, $t_{0.05m}(T_j)$ is the time needed for 5% precipitation at temperature T_j. The left hand side is accumulated over all roll passes. Siciliano and Jonas[9] concluded that the time for $t_{0.05m}$, for steel with additions of Mn and Si should be

$$t_{0.05m} = \frac{t_{0.05p}}{10^{(-0.26-0.90Mn+2.855Si)}} \qquad (7)$$

where $t_{0.05p}$ is the corresponding time for the isothermal strain-induced precipitation of Nb(C,N) according to [9,25]

$$t_{0.05p} = \frac{((\frac{Mn}{Si})^{0.42} e^{\frac{0.42\,Nb}{C}})}{169400} [Nb]^{-1} \frac{1}{\varepsilon_1^p} (\dot{\varepsilon}_1^p e^{\frac{Q_{def}}{RT}})^{-0.5} e^{\frac{Q_{di}}{RT}} e^{\frac{B}{T^3 (\ln(K_s))^2}} \qquad (8)$$

where R is the gas molar constant 8.314 [J/mol/K] and T is temperature [K]. B, Q_{def} and Q_{di} are constants, B=2.5·10^{10} [K^3], Q_{def} = 400 [kJ/mol] [11,25], Q_{di} = 270 [kJ/mol] [9,25]. K_s is the supersaturation ratio proposed by Irvine[27] K_s decides the driving force for precipitation. K_s can be obtained by[9]

$$K_s = \frac{10^{2.26-\frac{838Mn^{0.246}-1730Si^{0.594}-6440}{T_{rh}}}}{10^{2.26-\frac{838Mn^{0.246}-1730Si^{0.594}-6440}{T}}} \qquad (9)$$

where T_{rh} is the reheat temperature [K] applied before the plate is rolled.

2.3.2 Recrystallization and grain growth

The model first determines whether MDRX occurs during the reduction and also SRX after the rolling pass. X denotes the recrystallized fraction of the material. The grain growth is assumed to start when the recrystallisation is complete, taken as $X > 0.99$.

This recrystallized fraction of the material will have a low plastic strain. The fraction that recrystallized during a pass should then be followed separately with its own accumulated plastic strain. This is avoided in the current work in order to have an efficient model. The plastic strain computed according to Eq. (4) is therefore reduced as described below when recrystallization occurs. This is compensated by resetting X to zero after each roll pass, since the material is plastic deformed and the recrystallization starts from these new conditions. The plastic strain is assumed to be homogeneous over the cross section in every pass, the cross section is numerical treated as one fraction.

A more detailed model would follow the recrystallized fraction in each pass during later passes and with separate tracing of the plastic strain in this fraction.

The factors that determine influence on the recrystallization are steel grade, temperature, strain rate, strain and current grain size[13]. The evolution of the recrystallisation is assumed to follow the Avrami equation:

$$X = 1 - e^{(-0.693(\int \frac{dt}{t_{0.5}})^n)} \quad (10)$$

where $t_{0.5}$ is the time for 50 % for SRX or MDRX and n is a constant. For static recrystallization[11] n is 1, and 1.06 for metadynamic recrystallization[17]. Each of the models are evaluated and their contributions to X are added. The additivity rule was shown in ref.[11] to be a good approximation for solving the equation, since the plate cools down in the interpass times and the equations for $t_{0.5}$ are derived under isothermal conditions. The cooling curve is divided into steps each with constant temperature and the integral is taken over the roll pass time. The time steps are 0.001 [s] for MDRX and 0.1 [s] for SRX. The $t_{0.5}$ in eq.(10) is different for SRX and MDRX. The change in temperature during the interpass time is considered in the expressions using the temperature, but not the change of any further parameters in these expressions. The time for 50% MDRX, $t_{0.5MDRX}$ is determined by the formula derived in[17]:

$$t_{0.5MDRX} = 6.3 \cdot 10^{-4} d_0^{0.4} \varepsilon_1^{p\,-0.4} e^{(\frac{Q_{MDRX}}{RT})} \quad (11)$$

where Q_{MDRX} is the activation energy taken as 67 [kJ/mol] and d_0 [µm] is the entry austenite grain size in the pass.

MDRX is assumed to occur only if ε_1^p exceeds a critical strain ε_c determined as[9]

$$\varepsilon_c = \left(0.8 - 13Nb_{eff} + 112Nb_{eff}^2\right)\varepsilon_p \quad (12)$$

where ε_p is the peak strain from a true stress-strain curve for the material. Nb_{eff} gives the effect of niobium.

Extensive works[9,15-17] have been done regarding the effect of niobium and titanium on the recrystallization of the austenite. The observations indicate that niobium in solid solution has a retarding effect. The effective Nb content is determined as[9]

$$Nb_{eff} = Nb - \frac{Mn}{120} + \frac{Si}{94} \quad (13)$$

The relation has been determined for composition ranges of Nb 0.010-0.058 %, Mn 0.35-1.33 % and 0.01-0.23 % Si.

The peak strain ε_p was assumed for a Nb-Ti steel[18] to be possible to compute by the relation

$$\varepsilon_p = 3.7 \cdot 10^{-3} \frac{1 + 20 \cdot Nb + 0.02 \cdot Ti}{1.78} d_0^{0.147} Z^{0.155} \quad (14)$$

where Z is the Zener-Hollomon parameter

$$Z = \dot{\varepsilon}_1^p e^{\frac{Q}{RT}} \quad (15)$$

where the deformation activation energy Q is 325 [kJ/mol].

The static recrystallization occurs between the rolling passes provided it is not prevented by precipitation as discussed earlier. The time for 50 % SRX $t_{0.5SRX}$ for a Nb-Ti steel is determined by the formula derived by Fernandez and co-workers[16]

$$t_{0.5SRX} = 9.92 \cdot 10^{-11} d_0 \varepsilon_1^{p\,\{-5.6*d_0^{-0.15}\}} \dot{\varepsilon}_1^{p\,-0.53} e^{(\frac{180000}{RT})} e^{(\frac{275000}{T} - 185)(Nb + 0.374*Ti)} \quad (16)$$

The grain size is affected by the recrystallization and grain growth. The latter is only applied when the recrystallisation is complete. It is possible to have a partially recrystallized microstructure after a pass if the recrystallisation is not complete when the interpass time stops. Then the new grain size d_1 is determined as an average of the entry grain size d_0 and the grain size $d_{MDRX\ or\ SRX}$ of the recrystallized fraction after MDRX or SRX:

$$d_1 = (1 - X)d_0 + X \cdot d_{MDRX\ or\ SRX} \quad (17)$$

The metadynamically recrystallized grain size d_{MDRX} is mainly dependent on the strain rate and temperature[17,18]. According to Fernandez and co-workers, d_{MDRX} can be described as[18]:

$$d_{MDRX} = 812 \cdot Z^{-0.13} \quad (18)$$

where the Zener-Hollomon parameter Z is obtained from Eq. (15).

Thereafter static recrystallisation may occur. A corresponding formula as Eq. (16) is then applied where d_{MDRX} is replaced by d_{SRX}. The exit grain size d_{SRX} in the static recrystallized fraction computed as[19]

$$d_{SRX} = Kd_0^m \varepsilon_1^{p\,-v} \quad (19)$$

where K, m and v are material dependent constants[11,12,20]. The values are K=1.4, m=0.56 and v=1 in[11] for Nb-Ti steel. They are K=1.1, m=0.67, v=0.67 in[12] and K=0.5, m=0.67, v=1 in[20] for C-Mn-steels. In this study the values of K, m and v has been determined from the full-scale experiments giving K=1.3, m=0.65 and v=0.67. See the section about the full-scale experiments.

The material is assigned an entry plastic strain ε_0^p in the last time increment of any interpass time. This entry plastic strain is used in Eq.(4). The model is updated with following expression

$$\varepsilon_0^p = \lambda(1 - X)\varepsilon_1^p \quad (20)$$

where λ is a constant, reported to fall between [0.5-1][10,12,21]. In this work λ =1 is used.

Grain growth is accounted for when the recrystallization is complete (X>0.99). It is assumed to follow the equation[10]:

$$d_1^u = d_{MDRX\ or\ SRX}^u + kte^{\left(\frac{-Q_g}{RT}\right)} \quad (21)$$

where t [s] is the time after the recrystallization is completed. Q_g is the apparent activation energy for growth, u is the growth exponent, and k is a constant. Different values of u and k have been reported depending on the steel grade[17, 22]. Minami and co-workers[22] set that u= 4.5, k=4.1·10^{23} [1/s], and Q_g= 435 [kJ/mol] for Nb-steels. In[17], u=7, k=1.31·10^{18}[1/s], Q_g =172 [kJ/mol] for SRX and u=7, k=4.32·10^{19} [1/s] and Q_g =217 [kJ/mol] for MDRX. Different values of m, k and Q_g were tested in the pass schedule generator. Good agreement was obtained, for u=7, k=9·10^{25} [1/s], Q_g =435 [kJ/mol] for both SRX and MDRX. Eq. (21) was also solved with the additivity rule.

2.3.3 Model for final ferrite grain size

The ferrite size can be expressed as a function of the austenite grain size, retained strain, chemical composition and cooling rate[23]. The cooling rate is controlled by the amount of accelerated cooling in Oxelösund. According to Gibbs and co-workers, the strongest influence on the ferrite grain size is the amount of retained strain[24]. A relationship between the final ferrite grain size d_α and the influencing parameters is[24]

$$d_\alpha = (1 - 0.8\varepsilon_1^{p\,0.15})(29 - 5\sqrt{\dot{T}} + 20(1 - e^{-0.015d_1})) \quad (22)$$

where ε_1^p is the retained strain when the cooling starts, $\dot{T}$ [°C /s] is cooling rate, d_1 [µm] is the austenite grain size. The cooling rate was set to 0.5 [°C /s] during the final cooling of the plate after rolling corresponding to air cooling for 70 mm plate and 2.5 [°C /s] for 40 mm plate. This is the ferrite grain size that would be obtained if the plate with the current austenite grain size and plastic strain is cooled to room temperature.

3 Experiments for calibration and validation of the model

3.1 Experiments for the austenite grain size

The experiments were used to calibrate the parameters *K*, *m* and *v* in Eq, (19). Four steel plates were rolled in the four-high mill in Oxelösund and cooled in the equipment for accelerated cooling in order to investigate the austenite grain size. All plates were rolled with short interpass times, in the range of 5-15 [s] between the passes. Their detailed chemical compositions are displayed in **Table 1**. The silicon content of the steels in the experiments were outside the composition range for Eq. (7) but it is assumed that the equation can be used also for these steels.

The pass schedules for the experiments are shown in **Table 2**. The reheat temperatures were around 1160°C.

3.2 Experiments for the ferrite grain size after TM-rolling

Another set of experiments was carried out at a laboratory mill at MEFOS[29)] where the ferrite grain size was measured after cooling to room temperature. These tests were used to validate the ferrite prediction of the model, which is the crucial item in the model. **Table 3** shows the chemical compositions of the rolled specimens and **Table 4** shows the pass schedules.

3.3 Measurements of grain sizes

Probes were cut from the full-scale rolled plates in **Tables 1** and **2**. The measurements of austenite grain size were obtained by polishing and etching with Bechet-Beaujard. This reveals the prior austenite grain boundaries. The structures were photographed at locations in the thickness directions that were a quarter of the thickness and in the center of the plates. Five photos were taken on each depth. Theses pictures were used for a compare analysis and two intercept analyses per probe. The five pictures were compared to standardized pictures of structures, and an average ASTM-value was received. The mean width and mean height of approximately 100 grains per direction were determined. The measurements gave mean intercept values and corresponding ASTM-value in the horizontal rolling direction and an intercept in the vertical thickness direction, respectively. The average grain size on each depth was also determined as the half of the horizontal intercept plus the half of the vertical intercept.

The image analysis system µGOP 2000/s has been used in order to determine the ferrite grain size for the cases in **Tables 3** and **4**. More than 1100 grains have been measured in each sample[29)].

3.4 Calibration of model

The full-scale experiments were used to calibrate the full-scale generator. A comparison between measurements of the full-scale experiments and simulations was used in order to determine the parameters *K*, *m*, *v* and *k* in eq.(18, 21). K=1.3, m=0.65 and v=0.67, $k=9\cdot10^{25}$. After this calibration, no more adjustments of the microstructure model were done. The horizontal, vertical, average and simulated austenite grain sizes for the four different experiments are listed in **Table 5**.

Five pictures were taken from the test pieces and compared on every depth

The recrystallization regime was only static in number case 1, 2 and 4 as no precipitation occurred. MDRX occurred after the fifth pass of case 3. The simulations showed that the temperature has a great influence on the microstructure. It is important that the temperature calculations are accomplished with high precision, to ensure accurate material properties.

3.5 Validation of model

The proposed model is validated by comparing the predicted ferrite grain sizes with the measured ones from the experiments summarised in **Tables 3-4**. The results are also compared with predictions for plate rolling by the program MicDel, listed in[29]. The reason for the comparisons with MicDel is that MicDel is established software and is considered as a good method for microstructure analyses[29]. The MicDel model is based on semi-empirical equations for volume fraction of recrystallized austenite and recrystallized austenite grain size according to eq. (23), (24) and (25):

$$X = 1 - e^{(-k_{Micdel}(\frac{t}{t_{0.5}})^n)} \quad (23)$$

$$t_{0.5SRX} = Ad_0^a \varepsilon_1^{p^{\{-b\}}} Z^{-c} e^{(\frac{Q_{rex}}{RT})} \quad (24)$$

$$d_{SRX} = Bd_0^d \varepsilon_1^{p^{-e}} (e^{\frac{Q_d}{RT}})^{-f} \quad (25)$$

where X is the volume fraction of recrystallized austenite at the time t after deformation, $t_{0.5SRX}$ is the time for 50 % static recrystallization, d_{SRX} is the recrystallized austenite grain size. The constants k_{MicDel}, n, A, a, b, c, B, d, e and f are unique for each steel and dependent on its chemical composition. The pass schedule and the material coefficients for recrystallization are given in the input. The output is the calculated average austenite grain size and the ferrite grain size[30]. MicDel was practically applied on different kinds of steels with series of fitting parameters gained from laboratory results. The result is listed in **Table 6**. That should be pointed out, that the initial austenite grain size d_0 =20 [µm] in the MicDel-calculations[29]. The used value of 200 [µm] in the current developed software is more reasonable as the reheat temperature was in the same range as at normal full-scale rolling. MicDel calculates a finer ferrite grain size than the pass-schedule generator. The assumed finer initial austenite grain size in[29] contributes to finer final grain size. The pass-schedule generator results in finer grain size for the two 40 mm plates and coarser grain size for the 70 mm plate than measured. On the whole, the results from the proposed model in this investigation are in good agreement with the µGOP-measurements and even better than the MicDel-results.

4 Application of model

Pass-schedules for a slab of initial thickness 220 mm that should be given a final thickness 20 mm and width 2196 mm were determined by the roll pass scheduler as a demonstrator case. The chemical analysis was the same as for case 3 in the full-scale experiments. The reheat temperature was simulated as 1174°C. One pass-schedule without any long interpass time was also simulated as a reference case. The results are compiled in **Table 7.** Different length of the long interpass time were tested and also the amount of the pre-deformation before the long interpass time. The maximal length of this time was set to ten minutes and placed after the fourth pass. After rolling, two cooling rates are used, $\dot{T}$ =5 [°C /s] and $\dot{T}$ =10 [°C /s]. The latter corresponds to the ACcelerated Cooling (ACC) procedure. The plates rolled with five or ten minutes long delay time are affected of precipitation during the delay time and MDRX in the finishing rolling. This contributes to the very fine ferrite grains in these cases. It can be seen that the smallest ferrite

grain size is predicted for the case with four passes before the delay time and using a length of ten minutes. The decrease in temperature due to a long pause leads also to higher rolling forces. This requires more roll passes with less reduction in each pass. One can also observe, that even a pause length of one minute results in smaller ferrite grains compared to the reference pass schedule. Thus, the results show that the amount of pre-deformation and the delay time should be carefully chosen, to avoid unnecessary low productivity or on the other hand, to ensure a proper ferrite grain size in the finish rolled material. The software gives the possibility to find a length of the interpass time that reduces grain size without increasing the forces so that maximum reduction can not be applied in each pass. **Figure 3** illustrates how the austenite grain size changes during the TM-pass schedule for the plate with 5 minutes long delay time. The austenite grain size decreases rapid after the first passes, during the delay time grain growth occurs and the precipitation reaches 5 %. MDRX occurs in the second pass after the delay time.

5 Discussion

The proposed roll pass scheduler is an improvement of existing software for planning of roll pass schedules at the heavy plate mill at SSAB in Oxelösund. The software consists of a number of more or less advanced models. The proposed models for the material behavior were chosen from different sources, in order to obtain accurate description for the actual steel grades. The motivation for the development of the software is the need for a code that is possible to use on-line. Therefore, the existing MicDel was not an alternative for the complete investigation. Moreover, neither precipitation of Nb(C,N) nor MDRX are considered in MicDel. The model for the yield limit in Eq. (3) is important for the force calculations. It is obvious that it does not contain any direct influence of the austenite grain size. There are also open issues about the effect of precipitation on the recrystallisation.
Cho and co-workers observed that precipitation could not prevent dynamic recrystallization[26]. The precipitation model and Eq.(12) were extrapolated for some steel grades in the investigation with respect to the compositions of Mn and Si. The used models are however more accurate than then original model proposed of Dutta and Sellars in[25]. The models were tested on a number of chemical compositions in[9] with acceptable results.
The model assumes homogenous and isotropic conditions over the thickness of the plate and only predicts one grain size. In reality the austenite grain sizes vary over the thickness of the plate. They are also more elongated in the rolling direction. However, the observed variations are small in the most cases, see **Table 5**. Zheng established that uniform and fine ferrite grains of 6 µm can be achieved using recrystallization controlled rolling[14]. Morrison[2] found out that ferrite grain sizes of ~5 µm may be obtained in thin plates of commercially controlled-rolled micro alloyed steels[2].
This investigation demonstrates in **Table 7** the difficulty to reach a fine-grained ferrite microstructure. Achieving a ferrite grain size of 5-6 µm needs a careful investigation of the pass-schedule before the full-scale production starts, to secure proper ferrite grain size and avoid unnecessary low productivity due to long delay time. Longer delay time and lower finishing rolling temperature promotes finer ferrite grain size.

Acknowledgements

Jernkontoret - the Swedish Steel Producers' Association, and the Knowledge Foundation which both supported the project, are fully acknowledged.

6 References

1) B. Ahlblom: Proc. of Stålindustrins värmnings-bearbetnings och materialpaket 1999-2003, Borlänge 27-28 Oct. 2003, report D 797, project 31042, Swedish Steel Producers' Association, Stockholm, (2003), 4.

2) W. B. Morrison and J. A. Chapman: Controlled rolling, British Steel Corporation, GS/PROD/MISC/107/75/C, (1975), 1.

3) A. Köthe, J. Richter, A. Güth, L. Kaun, G. Backmann, M. Schaper and U. Gutteck: Recrystallization-controlled rolling of C-Si-Mn-V-N steel, Institut für Festkörper- und Werkstofforschung Dresden, Germany, (1989).

4) B. Leden: User's Manual STEELTEMP®, MEFOS Metal Working Research Plant, Sweden, (1997).

5) J. Levén: User's Manual CROWN426, MEFOS Metal Working Research Plant, Sweden, (2004).

6) T. Nilsson, P. Huml, U. Ståhlberg, T. Engelbert, S. Essle, K. Larsson and U. Öhman: Massivomformning, Verkstadstekniska processer, Tribologi, Formelsamling, Institution for metal working, Royal Institute of Technology, Stockholm, (1986).

7) T. Senuma and H. Yada: Proc. of Int. Symp. on Accelerated Cooling of Rolled Steel, Pergamon Press, New York, (1988), 105.

8) J. G. Beese: Iron Steel Eng., 57 (1980), 49.

9) F. Sicilliano and J. J. Jonas: Metall. Mater. Trans A, 31A(2000), 511.

10) C. M. Sellars and J. A. Whiteman: Met. Sci., 13(1979), 187.

11) R. Abad, A. I. Fernandez, B. López and J. M. Rodriguez-Ibabe: ISIJ Int., 41(2001), 1373.

12) C. M. Sellars: Mater. Sci. Technol. 6(1990), 1072.

13) T. Siwecki and G. Engberg: Proc. of Thermo-Mechanical Processing in Theory, Modelling & Practice [TMP] exp 2, Stockholm, 4-6 Sept. 1996, Swedish Society for Materials Technology, (1997), 121.

14) Y. Z. Zheng, A. J. DeArdo, R. M. Fix and G. Fitzsimons: Proc. of HSLA Steels Technology and Applications; Philadelphia, 3-6 Oct. 1983, American Society for Metals, (1984), 85.

15) J. Zrnik, T. Kvackaj, A. Pongpaybul, P. Srcharoenchai, J. Vilk and V. Vrovinsky: Mater. Sci. Eng. A, A319-321(2001), 323.

16) A. I. Fernandez, P. Uranga, B. López and J. M. Rodriguez-Ibabe: ISIJ Int., 40(2000), 899.

17) S. I. Kim, Y. Lee, D. L. Lee and Y. C. Yoo: Mater. Sci. Eng., A355(2003), 390.

18) A. I. Fernandez., P. Uranga, B. López and J. M. Rodriguez-Ibabe: Mater. Sci. and Eng., A261(2003), 367.

19) C. M. Sellars: Proc. of Int. Conf. Hot Working and Forming Processes, Met. Soc., London (1980), 440.

20) C. P. Hong and J. J. Park: Mater. Proc. Technol.: 143-144(2003), 759.

21) L. P. Karjalainen, T. M. Maccagno and J. J. Jonas: ISIJ Int. 35(1995), 1523.

22) K. Minami, F. Siciliano, T. M. Maccagno and J. J. Jonas: ISIJ Int. 36(1996), 1507.

23) Y. T. Zhang, D. Z. Li and Y. Y. Li: Acta Metatallurgica Sinica, 15(2002), 267.

24) R. K. Gibbs, B. A. Parker and P. D. Hodgson: Proc. of International Symposium on Low-Carbon Steels for the 90's; Pittsburgh, 18-21 Oct. 1993, Recrystallization'90, ed. By T. Chandra, The Minerals, Metals & Materials Society, USA (1993), 173.

25) B. Dutta and C. M. Sellars: Mater. Sci. Technol. 3(1987), 197.

26) S. H. Cho, K. B. Kang and J. J. Jonas: ISIJ Int. 41(2000), 63.

27) K. J. Irvine and F. B. Pickering: Iron Steel Inst., 205(1967), 161.

28) D. Q, Bai: PhD Thesis, McGill University, Montreal, (1995), 28.

29) T. Siwecki and O. Wang: Microstructure evolution during energy saving heavy plates RCR rolling of Ti-V microalloyed steel, Swedish Institute for Metals Research, Research Report no: IM-2003-565, (2003), 1.

30) P. Hansson: PhD Thesis, Institution for industrial production, Royal Institute of Technology, Stockholm (2004), 45.

7 Appendix

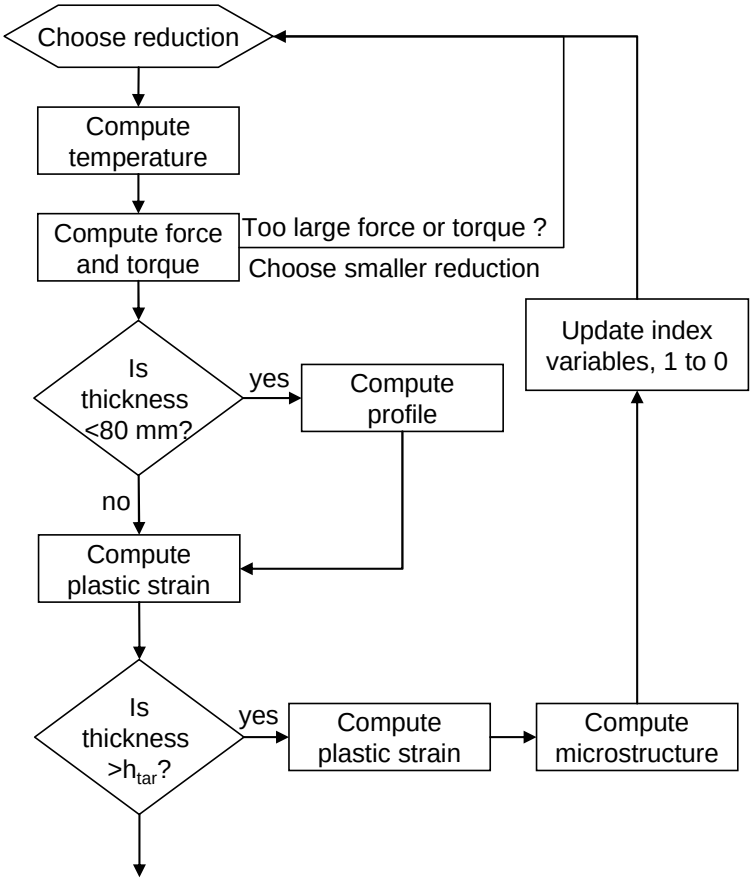

Figure 1. *The flow chart for each rolling pass of the roll pass schedule generator.*

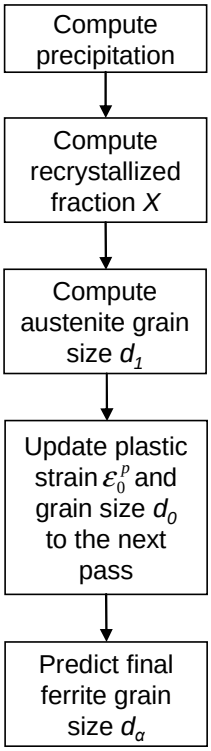

Figure 2. *The flow chart of the microstructure model.*

Table 1. Chemical compositions of the steels (in mass%) for the austenite grain size experiments.

Case	**C**	**Mn**	**Mo**	**Cr**	**Nb**	**Si**	**Ti**	**V**
1	0.135	1.007	0.153	0.252	0.015	0.342	0.010	0.020
2	0.131	1.006	0.156	0.258	0.015	0.300	0.010	0.017
3	0.136	0.996	0.143	0.241	0.015	0.286	0.009	0.019
4	0.133	1.029	0.150	0.241	0.016	0.307	0.010	0.020

Table 2. *The basics of the pass schedules in the full-scale experiments on plates in Table 1.*

Case	Total number of working passes	Reheat temperature	Slab thickness [mm]	Final thickness [mm]	Exit temperature from the last pass	Time from furnace to start of cooling after rolling
1	11	1169°C	220	12.0	1027°C	4 min 6 s
2	12	1174°C	220	14.0	1024°C	4 min 3 s
3	10	1174°C	220	12.0	1061°C	3 min 21 s
4	11	1167°C	220	12.0	1013°C	3 min 35 s

***Table 3**. Chemical compositions of the steels (in mass%) for the ferrite grain size experiments.*

Case	**C**	**Mn**	**Mo**	**Cr**	**Nb**	**Si**	**Ti**	**V**
5	0.132	1.51	--	--	0.001	0.46	0.011	0.046
6	0.151	1.45	--	--	0.001	0.46	0.010	0.046
7	0.132	1.51	--	--	0.001	0.46	0.011	0.046

***Table 4.** The basics of the pass schedules rolled in the four-high reversible rolling mill at MEFOS.*

Case	Total number of working passes	Reheat temperature	Slab thickness	Final thickness	Time from start of rolling to the last pass	Delay time	Reduction after the delay time
5	10	1160°C	220 mm	40.5 mm	4 min 50 s	3 min 15 s	12.7 %
6	10	1164°C	220 mm	40.4 mm	5 min 21 s	4 min 17 s	13.0%
7	7	1150°C	220 mm	71.4 mm	6 min 51 s	5 min 53 s	17.4%

***Table 5.** The horizontal, vertical, average and simulated austenite grain sizes for the plates.*

Case	Depth	Horizontal meanintercept [µm]	Vertical meanintercept [µm]	Average meanintercept [µm]	Simulated mean intercept [µm]
1	Center	26.9	23.5	25.2	23.0
1	t/4	21.2	21.0	21.1	
2	Center	24.5	24.7	24.6	23.3
2	t/4	22.5	25.3	23.9	
3	Center	25.4	20.5	22.9	25.0
3	t/4	22.7	20.2	21.5	
4	Center	24.2	20.7	22.4	21.5
4	t/4	20.4	16.5	18.4	

***Table 6.** The measured and simulated ferrite grain sizes for the rolling at MEFOS.*

Case	Measured ferrite grain size [µm]with µGOP[29)]	Calculated ferrite grain size [µm] with MicDel[29)]	Simulated ferrite grain size [µm] with the pass-schedule generator
5	14.3	9.6	12.7
6	14.7	8.3	12.6
7	12.3	10.1	14.9

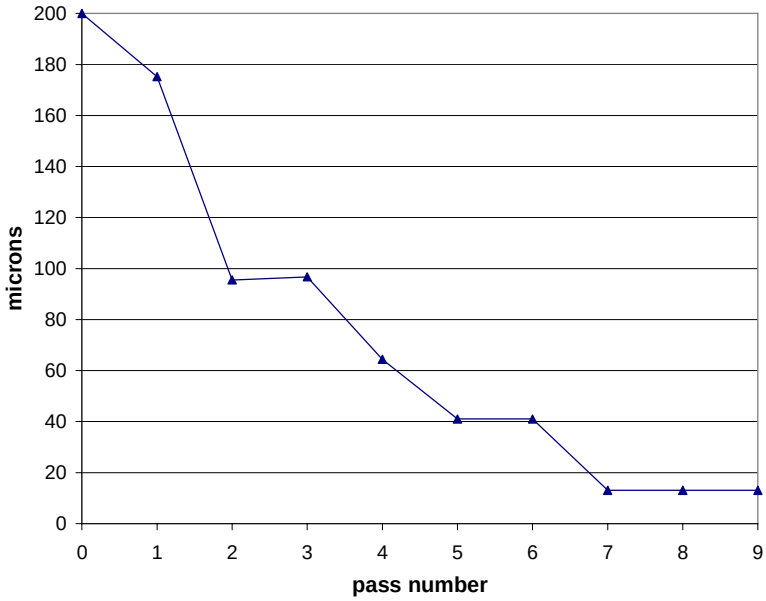

Figure 3. *The austenite grain size after every pass in the TM-pass schedule for the plate with 5 minutes long delay time. The initial austenite grain size is 200 µm before the first pass.*

Table 7. *Simulated results by the pass-schedule generator.*

Austenite grain size at start of ACC [µm]	29.8	24.1	13.1	10.9
Ferrite grain size [µm] after ACC	$\dot{T}$ =[5/s]:25.0 $\dot{T}$ =[10/s]:20.4	$\dot{T}$ =[5/s]:21.3 $\dot{T}$ =[10/s]:17.2	$\dot{T}$ =[5/s]:5.39 $\dot{T}$ =[10/s]:4.22	$\dot{T}$ =[5/s]:5.26 $\dot{T}$ =[10/s]:4.09
Accumulated strain before ACC [- -]	0	0	0.639	0.635
Number of passes before delay time	--	8	5	4
Length of the delay time [min]	--	1	5	10
Finishing rolling temperature	1092°C	982°C	929°C	895°C
Total number of passes	8	8	9	10
Type of rolling schedule	SRX+MDRX	SRX+MDRX	SRX+PRE+MDRX	SRX+PRE+MDRX

B

Modeling the work roll wear contour in a four-high mill

Mikael JONSSON
SSAB Oxelösund AB, GVT 7013, SE-613 80 Oxelösund, Sweden.
E-mail: mikael.jonsson@ssabox.com

Abstract
A method for modeling of the work wear roll contour in a four high mill has been developed. The method is a combination of simple models calibrated with statistical methods. The bases for the statistics are simulations of different rolling cases and measurements from the production of heavy plates in Oxelösund. These calibrations gave a well-working model.
KEY WORDS: wear, wear model, statistic model, roll simulation, specific rolling force, rolling pressure.

1 List of symbols

F	rolling force, N
B	work roll bending force, N
G	sum of roll gravity load and roll balancing force, N
W	width of the rolled material, mm
h_0	entry thickness, mm
h_1	exit thickness, mm
x	position along the work roll barrel related to the edge of the roll
x_1	relative position along the work roll barrel related to the workpiece
x_2	relative position along the work roll barrel related to the back-up roll
$C(x)$	roll wear along the barrel length as function of x, mm
C_e	local wear at the edge of the plate, mm
C_m	absolute local roll wear in the middle of the plate, mm
c_s, c_1, c_2, k_w, k_1, k_2, exp_1, exp_2	empirical coefficients that depend on material of roll and workpiece and etc.
L_{plate}	length of the rolled material in a pass, mm
v_1	Poisson's ratio for the work roll material
v_2	Poisson's ratio for the back-up roll material
E_1	modulus of elasticity for the work roll material, MPa
E_2	modulus of elasticity for the back-up roll material, MPa
R_1	nominal radius of the work roll, mm
R_d	flattened radius of the work roll according to Hitchcook, mm
R_2	nominal radius of the back-up roll, mm
l_{d-1}	contact length between the work roll and plate, mm
l_{d-2}	contact length between the work roll and the back-up roll, mm
L_b	nominal barrel length of the back-up roll, mm
$L_{b\text{-}real}$	barrel length of the back-up roll in contact with the work roll, mm
$P_1(x_1)$	force per unit length between the rolled material and the work roll as function of x_1, N/mm
$P_2(x_2)$	force per unit length between the back-up roll and the work roll as function of x_2, N/mm
$Q_1(x_1)$	pressure between the rolled material and the work roll as function of x_1, MPa
$Q_2(x_2)$	pressure between the back-up roll and the work roll as function of x_2, MPa
T_{entry}	Entry crown of the plate in the pass, mm
T_{exit}	Exit crown of the plate in the pass, mm
ε	plastic strain due to reduction in the pass = $\ln(h_0/h_1)$

2 Introduction

As a result of the high energy consumption in the modern society, demands have arisen from different markets to reduce it. Especially, the transportation sector can achieve large energy savings by weight reductions. The extra and ultra high strength structural steels and abrasion resistant steel are suitable materials in many designs, since mild steel can be replaced with thinner material. The rolling technique of thin and wide plates in a reversible four-high heavy plate mill is complicated, particularly the flatness control, due to the low plate stiffness.

There are a number of factors affecting the flatness. One of these factors is the wear contour of the work rolls. The schedule-free planning of the production mix and the modern roll shifting technique, increase the need for accurate calculation models for prediction of the roll wear contour. Therefore, knowledge of the current wear contour is important to determine during the rolling, since the flatness control may lead to reduction limits during the pass schedule. In addition the axial roll shifting position and the amount of dynamic work roll bending can be accurately predicted.

The aim with this work is to establish an accurate and fast on-line method to predict the wear contour of the work rolls in the four-high mill in Oxelösund. The basic models used in the current work are development of models from the literature with respect to the wear distribution along the roll. Design of experiments has been used to obtain a set of proper simulations of different passes in the mill. The results from these simulations were used in a regression analysis in order to calibrate the model for the load distribution across the rolling direction. A polynomial distribution of the load approximation has been used. The load distribution is fundamental for the determination of the wear contour. The wear model is calibrated with data from the full-scale production. See **Figure 1** for an overview of the approach used in the study.

2.1 Previous work

In hot rolling, the work rolls are subjected to periodic loading that is accompanied with abrasion by scale and fluctuations in temperature [1]. The wear process is a complex phenomenon and has several components [2]. There are four major causes of roll wear [3, 4]:

a) Abrasion of roll surface due to the contact with the rolled material and back-up rolls.
b) Mechanical fatigue of roll surface layer as a result of cyclical loading of the rolls.
c) Thermal fatigue of roll surface layers as they are periodically heated by the rolled material and cooled by water sprays.
d) Corrosion.

The abrasion and the fatigue are two primary types of wear for the work roll in plate rolling [5]. The two forms of roll wear that are generally recognized as overall and local [5]. The overall work roll wear is located over the entire length of the barrel subjected to thermal and mechanical fatigue, with corrosive wear playing a subordinate role [6]. The work roll wear is generally nonuniform [5]. The uneven wear of the surface of work roll is a major cause for influencing on the plate profile [7]. The roll wear can be described as local when the wear length along the barrel length is substantially less than the width of the rolled material [5]. The following two types of local work roll wear in hot rolling mills are observed:

a) Local roll wear near the edges of the plate, C_e.
b) Local roll wear between the plate edges, C_m.

The local wear near the edges of the plate, is a result of the higher rolling pressure there due to the discontinuity which the plate edges cause.

A wear model developed by Nakanishi [8], assumes that C_e is proportional to C_m:

$$C_e = kC_m \qquad \text{(1)}$$

where the wear increase coefficient $k \approx 1.3$ and depends on the geometric and material circumstances [8]. Ohe et al developed a model for prediction of C_m [9]:

$$C_m = c_1\left(\frac{L_{Plate}}{R_1}\right)\left(\frac{F}{W \cdot l_{d-1}}\right)^{1.77} + c_2\left(\frac{L_{Plate}}{R_1}\right)\left(\frac{F}{L_b}\right)^{0.5} \quad \ldots\ldots\ldots\ldots\ldots\ldots(2)$$

Thus, equation (2) takes the properties of both the work roll and the back-up roll into account, as well as the rolled material. The formula for the contact length l_{d-1} is:

$$l_{d-1} = \sqrt{R_d(h_0 - h_1)} \quad \ldots\ldots\ldots\ldots\ldots\ldots\ldots\ldots\ldots\ldots(3)$$

where R_d is obtained from the Hitchcock theorem for flattened work roll radius [10]:

$$R_d = R_1\left(1 + \frac{16(1-\nu_1^2)P_1}{(h_0 - h_1)\pi E_1}\right) \quad \ldots\ldots\ldots\ldots\ldots\ldots\ldots\ldots\ldots\ldots(4)$$

where **Figure 2** shows the definitions of l_{d-1}, h_0 and h_1.
Another wear model was proposed by Lixfeld [11]:

$$C_m = c_s \cdot \left(\frac{F}{W \cdot l_{d-1}}\right)^{0.3} \cdot \frac{L_{Plate} \cdot l_{d-1}}{R_1} \quad \ldots\ldots\ldots\ldots\ldots\ldots\ldots\ldots\ldots\ldots(5)$$

Equation (5) only considers the wear caused by the rolled material, which approximately corresponds to the first term in equation (2).
CROWN426 is a program package for simulating thickness profile and flatness in flat rolling. Work roll profile is calculated with models accounting for thermal expansion and wear. The elastic deformation of rolls and the deformation of the rolled material are calculated for both hot and cold rolling mills with 2-6 rolls. Simulation of 6-high mills with adjustable intermediate rolls and work rolls, 4-high mill with adjustable work rolls, 5-high mill with an extra roll adjusted in relation to the mill's symmetry line and other unsymmetrical mills can be performed with this software. Simulation of tandem mills with up to 7 roll stands is possible. The model takes into account strip tensions between roll stands and between the last stand and the coiler. Force distributions between rolls are calculated. The expression for calculation of the wear distribution, $C(x)$, in CROWN426 is [13]:

$$C(x) = k_w L_{plate} Q_1(x_1) \frac{\sqrt{1 + \dfrac{16Q_1(x_1)\dfrac{(1-\nu_1^2)}{\pi E_1}}{h_0 - h_1}}}{2\pi R_1} \quad \ldots\ldots\ldots\ldots\ldots\ldots\ldots\ldots\ldots\ldots(6)$$

The load distribution function $Q_1(x)$ due to the pressure between the work roll and the plate is introduced in order to handle both the overall and local wear. The drawback of the method is a time demanding simulation (~30 s. per pass) with CROWN426 to obtain $Q_1(x)$. CROWN426 does not include contribution to the wear from the back-up roll.

3 The rolling process and proposed wear models

Different types of extra and ultra high strength structural steels and abrasion resistant steels are rolled in the four-high mill in Oxelösund. A number of measured work roll profiles before and after rolling were collected. The data was taken from the roll grinder, during January 2005 to January 2006. Different campaigns of heavy plates were rolled, with respect to width, thickness, steel grade, rolling force, plate

length, diameters of work- and back-up rolls, the roll shifting in axial position, work roll bending, and plate crowns. The plate crown is defined as the middle thickness of the plate minus its thickness 100 mm from the edge, see **Figure 3**.

Measured process data has been used as far as possible in the investigation, otherwise calculated values from the process computer were used. The ranges over the used variables are listed in **Table 1**.

3.1 Proposed model for the work roll wear contour

Replacing the roll force in equations (2), (5) and (6) with load distributions due to interaction between work roll and plate, Q_1, and back-up roll and the plate, Q_2, results in two approaches for calculation of $C(x)$:

$$C(x) = k_1 \frac{L_{Plate}}{2\pi R_1}\left(Q_1(x_1)\right)^{\exp 1} + k_2 \frac{L_{Plate}}{2\pi R_1}\left(Q_2(x_2)\right)^{\exp 2} \quad \text{.....(7)}$$

$$C(x) = k_1 \frac{L_{Plate}}{2\pi R_1} l_{d-1}\left(Q_1(x_1)\right)^{\exp 1} + k_2 \frac{L_{Plate}}{2\pi R_1}\left(Q_2(x_2)\right)^{\exp 2} \quad \text{.....(8)}$$

It is possible to obtain the work roll pressures $Q_1(x_1)$ and $Q_2(x_2)$ [MPa] from the relation

$$Q_1(x_1) = \frac{P_1(x_1)}{l_{d-1}(x_1)} \quad \text{.....(9a)}$$

$$Q_2(x_2) = \frac{P_2(x_2)}{l_{d-2}(x_2)} \quad \text{.....(9b)}$$

where l_{d-2} is obtained by using of a Hertzian contact area [12] :

$$l_{d-2} = \sqrt{\frac{16P_0}{\left(\frac{1}{R_1}+\frac{1}{R_2}\right)\left(\frac{1-\nu_1^2}{E_1}+\frac{1-\nu_2^2}{E_2}\right)}} \quad \text{.....(10)}$$

3.2 Fundamental factors for the wear and simulations

There is a need to have a fast calculation of the load distribution in order to use the model on-line. Thus, the difficulty in this case is to calculate $P_1(x_1)$ and $P_2(x_2)$ in equation (9). $P_1(x_1)$ and $P_2(x_2)$ can be simulated with CROWN426 but this algorithm is too slow . The use of this code to devekop simpler and faster models is described in the chapters 3.3-3.4. The following factors affecting $P_1(x_1)$ are taken into account, derived from the literature [13]:

- rolling force F
- plate width W
- nominal work roll radius R_1
- strain due to the reduction in the pass ε
- entry crown of the plate T_{entry}
- exit crown of the plate T_{exit}

The following factors affecting $P_2(x)$ are taken into account [3]:

- rolling force F
- plate width W
- work roll bending force B,

- work roll radius R_1
- back-up roll radius R_2

The real contact length $L_{B\text{-}real}$ between the back-up roll and the work roll and is usually shorter than the nominal barrel length of the back-up roll. Since $L_{B\text{-}real}$ influences $P_2(x)$ as well as the wear position on the work roll, it is important to determine $L_{B\text{-}real}$ as accurate as possible. Also $L_{B\text{-}real}$ were evaluated with CROWN426. The following factors that are affecting $L_{B\text{-}real}$ are taken into account [13]:

- rolling force F
- plate width W
- work roll bending force B
- work roll radius R_1
- back-up roll radius R_2

3.3 Approximation of $P_1(x)$ and $P_2(x)$ with polynomials

Ohe et al. [9] stated that $P_1(x_1)$ is well expressed by a polynomial of the fourth degree:

$$P_1(x_1) = \frac{F}{W}(a_0 + a_2 x_1^2 + a_4 x_1^4), \quad 0 \le x_1 \le \frac{W/2}{W/2} \qquad \text{……..……(11)}$$

Ohe et al. [9] also stated that $P_2(x_2)$ can be expressed of a fourth order polynomial. It was also tested in this work. However, it was soon found that a polynomial of fifth degree is a better approximation in the most cases, than a fourth degree polynomial. So the fifth degree polynomial was chosen to express $P_2(x_2)$:

$$P_2(x) = \frac{F+B+G}{L_{B-real}}(b_0 + b_2 x_2^2 + b_3 x_2^3 + b_4 x_2^4 + b_5 x_2^5), \quad 0 \le x_2 \le \frac{L_{B-real}/2}{L_{B-real}/2} \qquad \text{…..(12)}$$

The reason for the choice of a fifth degree polynomial is that the better fit was obtained with it, than a four degree polynomial. It was assumed that the barrel is symmetrical on both sides of the center line of the workpiece and the back-up roll and that the plate was always centered in the rolling gap.

3.4 Design of experiments and multiple regression

Design of experiments (DOE) are used in this study to determine the parameters in equations (11) and (12). The "experiments" are in this case simulations by means of CROWN426 where force distributions are computed. The basic idea of the DOE approach is described below and the results is given later.
The design of experiments is a technique to organize the experimental work into a minimum of work input and a maximal information output. The strategy is to vary all factors simultaneously in a planned set of experiments. The importance of each factor and the interaction between them can be estimated.
The basic idea is to devise a small set of experiments, in which all pertinent factors are varied systematically. Each experiment gives results i.e. values response variables. The data collected from the experiments are used to estimate the coefficients of the model. The model represents the relationship between the response Y and the factors z_1, z_2 etc.
MODDE is a software for the generation and evaluation of statistical experimental designs. Different designs with linear or interaction models are available. Thereafter, these data are analyzed by means of multiple regressions. Partial Least Squares projection to latent structures (PLS) or Multiple Linear Regression (MLR) are options available in MODDE. Both PLS and MLR computes regression coefficients for each response. Thus Y is expressed as a function of the z's according to the selected model regardless if it is linear, linear plus interactions or quadratic. This gives a model relating the factors to the results,

showing which factors are important, and how their combinations also in influence the results. The model is then used to make predictions, e.g. how to set the factors to achieve desired results [14].

4 Results

4.1 Determination of load distribution

4.1.1 Design of simulations and fitting of equation (11) and (12)

MODDE was used to design two proper sets of passes for simulation with CROWN426 to obtain $P_1(x_1)$ and $P_2(x_2)$ during changing rolling conditions. All parameters were used in low or high level and in combination with each other. From the very beginning, the idea was to have two equations for $P_1(x_1)$, one equation for negative entry crown and another for positive entry crown, 19 simulations of each equation were considered. It was later clear, that one equation is able to handle both positive and negative entry crowns so the sets of pass simulations were merged. Moreover, some extra control simulations were manually also added to guarantee good accuracy in the most common passes. Totally 43 simulations were performed for $P_1(x_1)$ and 19 simulations were performed for $P_2(x_2)$.

4.1.2 Polynomial load distribution approximation

$P_1(x_1)$ and or $P_2(x_2)$ were obtained from every CROWN426-simulation and were used to fit equation (11) and (12). The fitted coefficients were determined by the program MODDE.

4.1.3 Modeling of $P_1(x)$ by a polynomial of four degree

An interaction model and MLR-analysis was used of to create the expressions for a_0, a_2, a_4 respectively since this technique resulted in the best fit. It means that the parameters and interactions of two parameters with significant effect were estimated. The significant parameters and interactions became following for $P_1(x_1)$:

- rolling force F
- plate width W
- nominal work roll radius R_1
- strain due to the reduction in the pass ε
- entry crown of the plate T_{entry}
- $W \cdot T_{entry}$
- $R_1 \cdot T_{entry}$
- $\varepsilon \cdot T_{entry}$

Thus T_{exit} was not found to have any significant influence on the load distribution but the entry crown T_{entry} is important since all interactions terms include T_{entry}. However, T_{entry} and T_{exit} is related and it is not possible to change the plate crown all too much in a pass. **Figure 4** contains the scaled and centered coefficients for a_0, a_2, a_4. The figure shows that the most important factor for both a_0, a_2 and a_4 is $W \cdot T_{entry}$. The deviation of the factor importance is however great between a_0, a_2 and a_4.

4.1.4 Modeling of P2(x) by a five degree polynomial and LB-real

PLS-analysis and an interaction model gave the best fit for b_0, b_2, b_3, b_4 and b_5. The significant parameters and interaction were found to be following for $P_2(x_2)$:

- rolling force F

- plate width W
- work roll bending force B
- $F \cdot W$

R_1 and R_2 do not influence $P_2(x_2)$. **Figure 5** shows that the most important factor is the interaction of F and W, $F \cdot W$. The reason is probably due to the relative slender proportions of the rolls, the magnitude and distribution of the rolling force is important for the deformation according to the theory of beam bending. The radii of the rolls are not varying in the same range as the plate width, and can treated as constant.

Also for modeling of $L_{B\text{-}real}$ the same simulations as for $P_2(x_2)$ were used. PLS-analysis and an interaction model resulted in the best fit. The significant parameters and interaction were found to be following for $L_{B\text{-}real}$:

- F
- W
- B
- $F \cdot B$
- $W \cdot B$

It is clear, that the models of $P_2(x)$ and $L_{B\text{-}real}$ are closely related as many parameters that are of importance for them are common. The differences are that the interaction of W and B is significant for $L_{B\text{-}real}$ but not the radii of the rolls, shown in **Figure 6**.

4.2 Simulation of the wear contour with equation (7) and (8)

The previous procedure gives the load distributions and then equation (7) and (8) are complete and the roll wear can be computed. The measurements from the grinder were used to fit the wear simulations. Different pairs of work rolls from different suppliers have been analyzed. The measured wear profiles of the work rolls from 13 campaigns were added; every profile consisted of 121 measure points along the barrel. Therefore, the roll barrel was discretized into 120 segments which correspond to 121 calculations points. The work roll axial shifting position was taken into account as well. Every campaign consists of 2100-6100 passes. The best fit was received with low values of *exp1* and *exp2*, *exp1*=0.3 and *exp2*=0.2. The reason is that high values of *exp1* and *exp2* result in poor fit for campaigns with many passes of extra low or extra high rolling pressure. Low values of *exp1* and *exp2* give good prediction of the overall amount of wear of the roll for varying campaigns. Thus, the simulated wear contour becomes also smoother than the measured. The average correlation coefficients for equations 7 and 8 are 96.4 % and 95. 9% for the upper work roll, respectively. The corresponding values from the lower work roll are 98.1 % and 97.8 %. It is derived from the thirteen campaigns of the calculated wear profiles and measured. This shows that equation (7) is slight better than equation (8). The wear contour is better described ±1000-1500 mm from the middle of the barrel and the slope ±1000 is also in better agreement than equation (8). The differences is however small. The calculations of the lower work roll wear are also in slight better agreement than the corresponding for the upper work roll. The lower work roll is significant more worn than the upper work roll after a campaign.
In general, it was found that the calculated values match well with the measured ones for both the upper and lower work roll. See **Figure 7** and **8** for a demonstration of the calculated and measured wear contour of campaign number 7, of the upper and lower roll respectively.

5 Discussions

The wear phenomenon in hot rolling has been subject for extensive studies and research through the years. According to Meng [15] has at least 182 wear equations been proposed until 1994. However, Tahir [16] stated 2003 that just a few models is interesting for use in a process control system in a rolling mill. Tahir also stated that the wear model presented in [9] can be used for on-line calculation of the wear in the middle of a work roll. The result of the literature study in this work, also found that the Ohe-model in [9] is a proper starting point for a new model of the wear along the roll barrel. The use of a basic physical model that explains the amount of wear as function of rolled length and rolling pressure and a statistical model for the complex load distribution cross the rolling direction has in this work been proved to be a strong combination. Furthermore, the full-scale approach has the benefit that the model gets calibrated from authentic conditions. Since the approach is partly derived from active service, the measurements from the roll grinder are critical for the result. However, the machine is daily used in the production and seems to work well. The tolerance limit is ±0.05 mm from the nominal value. The air temperature in the grinding hall is not allowed to change more than 1°C from the set-up value.

The most critical part of the wear contour model, is however the accuracy of equations (11) and (12). The approach of Ohe [9] that $P_1(x_1)$ is well approximated of a four degree polynomial, with missing coefficients of first and third degree. The first degree term is zero due to symmetric conditions. The third degree term was not considered of Ohe in [9] and this approximation seems to work well according to the current results. A demonstration is given in **Figure 9.** Ohe also proposed the same type of equation for $P_2(x_2)$ as well. This approximation was found to be unsatisfactorily. A more complex form, equation (12) was therefore used. See **Figure 10** for demonstration. Also here, the first degree term is zero due to symmetric conditions.

Calculation of the wear contour with equation (11) and (12) shows that both equations are overall of high quality with good numerical stability. The measured increase in wear that appears around ±700-900 mm from the middle of the barrel is not predicted by the models. It is believed that this wear increase is related to cold edges of the workpieces resulting in higher load at this location. This effect is not accounted for in CROWN426 and therefore the coefficients for $P_1(x_1)$ does not include this.

The assumption that the rolls are cold and without any previous wear is in reality valid only in the first pass after changing of both the work rolls and back-up rolls. After some campaigns, the back-up rolls will become worn. However, the prediction of the back-up roll wear profile makes it possible to account for this in the model although it was not done in the present work. The idle rolling in the mill was not taken into account, since CROWN426 cannot simulate rolling without material between the work rolls. The guide boards center the plate in the roll gap before every pass and therefore the assumption that the plate is centered is motivated. The steel grade and the temperature influence the mechanical properties of the scale and therefore the wear. These effects were not explicitly included in the model.

6 References

[1] C. L. Robinson and F. J. Westlake:" Roll Lubrications in Hot Strip Mills", Conf. Proc. of the First European Tribology Congress, London, Sept. 25-27, (1973), p. 389-398.

[2] J. T. Burwell: "Survey of Possible Wear Mechanisms", Wear, vol. 1, (1957), p. 119-141.

[3] C. L. Wandrei: "Review of Hot Rolling Lubricant Technology for Steel", ASLE Special Publication SP-17, American Society of Lubrication Engineers, Park Ridge, III., (1984).

[4] P.G. Stevens: "Increasing Work Roll Life by Improved Roll Cooling Practice", Journal of the Iron and Steel Institute, (1971), p. 1-11.

[5] V. B. Ginzburg: "High-Quality Steel rolling", International Rolling Mill Consultants, Inc., Pittsburgh, Pennsylvania, Marcel Dekker, (1993), p. 505-525.

[6] J. A. Schey: "Tribology in Metalworking: Friction, Lubrication and Wear", American Society for Metals, Metals Park, Ohio, (1983), p. 131-141.

[7] S. Lin, L. L. Bingman, Z. Xiang, „The applications of Simulated Annealing Algorithm to Improve Wear Models in Plate Mills", Conf. Proc., 44th MWSP, Vol. XL, (2002), p. 593-603.

[8] T. Nakanishi, T. Sugiyama, Y. Lida: "Application of Work Roll Shift Mill HCW Mill to Hot Strip and Plate Rolling", Hitachi Review, Vol. 34 No. 4, (1985), p. 153-160.

[9] K. Ohe, S. Kajiura, S. Simada, A. Mizuta, Y. Morimoto, T. Fujino, K. Anraku, "Development of Shape Control in Plate Rolling", METEC Congress 94, 2nd European Continuous Casting Conference, 6th International Rolling Conference, Conf. Proc, vol. 2, (1994),Germany, p. 78-85.

[10] J. H. Hitchcock: "Roll-neck bearings", ASME research publications, (1935)

[11] P. Lixfeld: "Functional description of Profile and Flatness Control", Specifications of the Plate Mill in Oxelösund, SMS Demag AG, Germany, (1996).

[12] B. Sundström: "Handbook of Solid Mechanics (in Swedish), Fingraf AB, Södertälje, Sweden, (1998), p. 127-130.

[13] J. Levén: "User Manual CROWN426" (in Swedish), MEFOS Metal Working Research Plant Sweden, (2004).

[14] Umetrics AB: "MODDE 7.0 User Guide and Tutorial", Umetrics AB, Umeå, Sweden, (2003).

[15] H.C. Meng: „Wear modeling: evaluation and categorization of wear models", Ph.D Thesis, University of Michigan, Ann Arbor, USA, (1994).

[16] M. Tahir: „Some Aspects on Lubrication and Roll Wear in Rolling Mills“, Ph.D Thesis, Division of Materials Forming, Department of Production Engineering, Royal Institute of Technology, Stockholm, Sweden, 2003, p.9-16.

7 Appendix

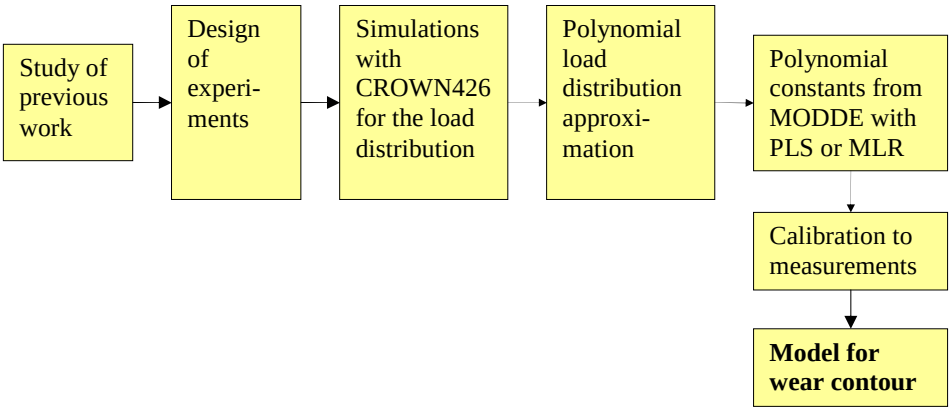

Figure 1. *Flow chart for development of the model for the work roll wear contour.*

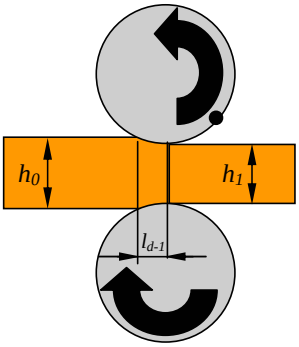

Figure 2*. View of the roll gap cross the rolling direction.*

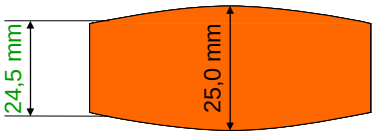

Figure 3. *Demonstration of the plate cross section and crown. The crown is 0.5 mm in this case.*

Table 1. *Basic conditions for the investigation.*

Range of rolling force F:	$9.81 \cdot 10^6$-$9.81 \cdot 10^7$ N	Range of work roll bending force B:	$1 \cdot 10^6$-$3.5 \cdot 10^6$ N per neck
Sum of balancing force and gravity force between lower work roll and back-up roll G	$3.158 \cdot 10^3$ N	Sum of balancing force and gravity force between upper work roll and back-up roll G	$2.243 \cdot 10^3$ N
Range of reduction ε:	1-60 %	Type of work roll shell, hardness:	HiCr, typically 16-18% chromium, 605 Vickers
Range of plate width:	900-3600 mm	Modulus of elasticity E_1 and Poisson's ratio ν_1 for the work roll shell:	E_1=210 000 MPa, ν_1=0.3
Range of work roll diameter R_1:	480-530 mm	Type of back-up rolls, modulus of elasticity E_2 and Poisson's ratio ν_2:	Forged steel, E_2=210 000 MPa, ν_2=0.33
Range of back-up roll diameter R_2:	975-1075 mm	Measured barrel length work rolls:	3630 mm
Range of entry plate crown T_{entry}:	-4-0.8 mm	Nominal barrel length of back-up rolls L_B:	3600 mm
Range of exit plate crown T_{exit}:	-4-0.8 mm	Range of work roll shifting in axial direction:	±150 mm

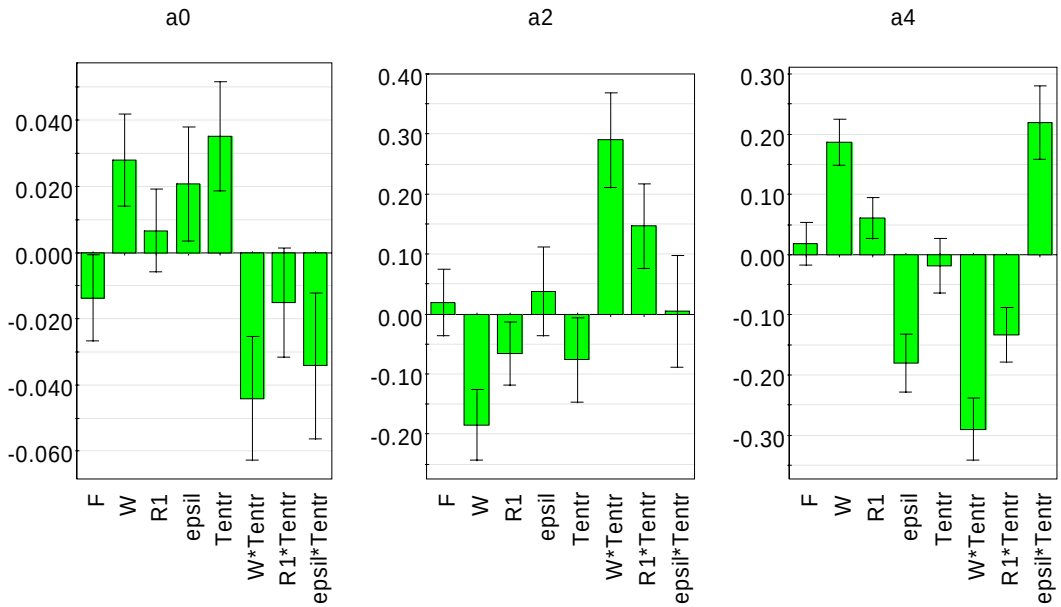

Figure 4*. Scaled and centered coefficients for a_0, a_2 and a_4 in equation (11)).*

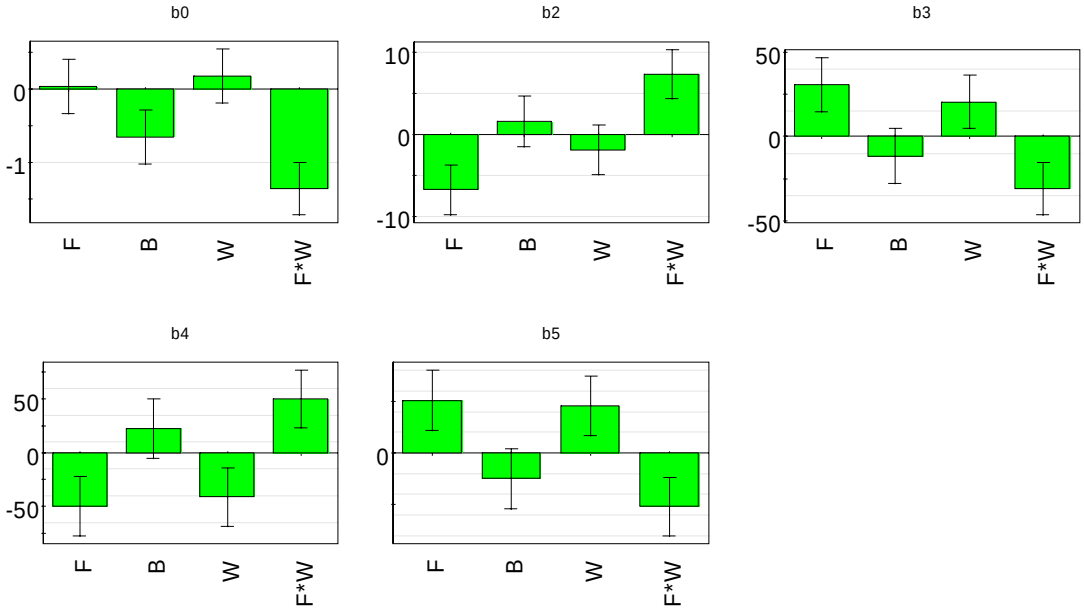

Figure 5. *Scaled and centered coefficients for b_0, b_2, b_3, b_4 and b_5 in equation (12).*

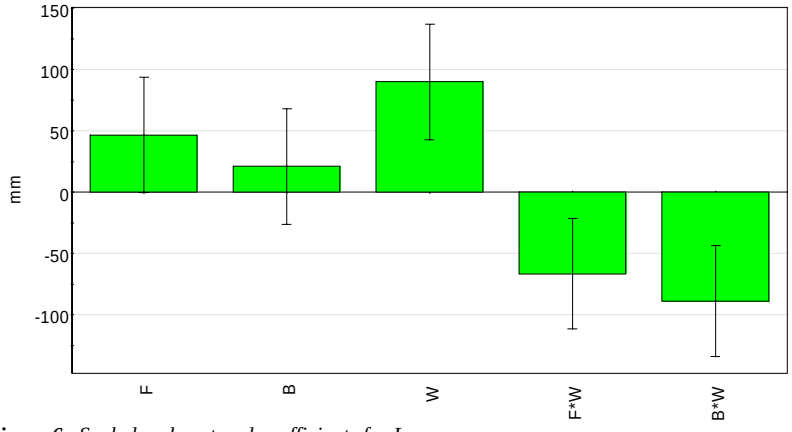

Figure 6. *Scaled and centered coefficients for $L_{B\text{-}real}$.*

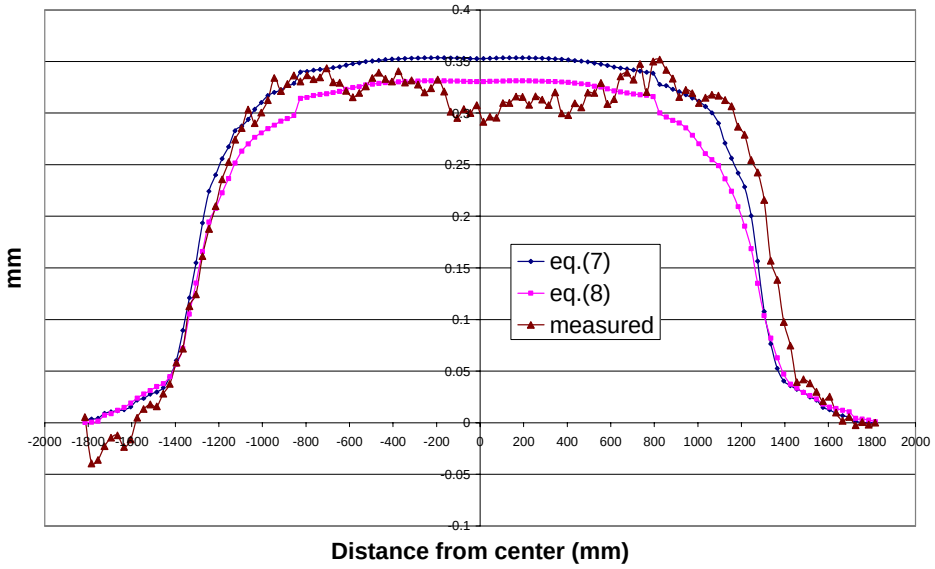

Figure 7. *Comparison of the simulated and measured wear along the barrel of the upper work roll after campaign number 7.*

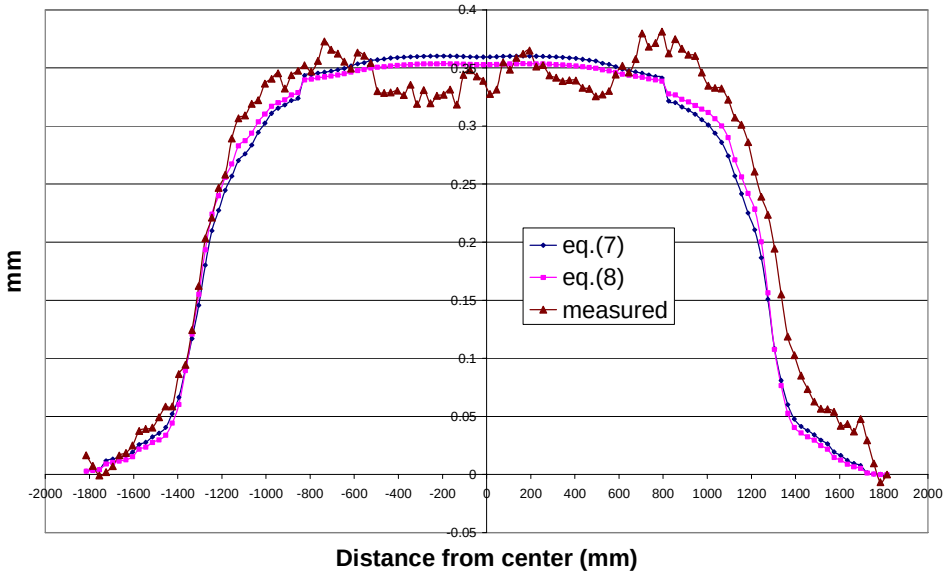

Figure 8. *Comparison of the simulated and measured wear along the barrel of the lower work roll after campaign number 7.*

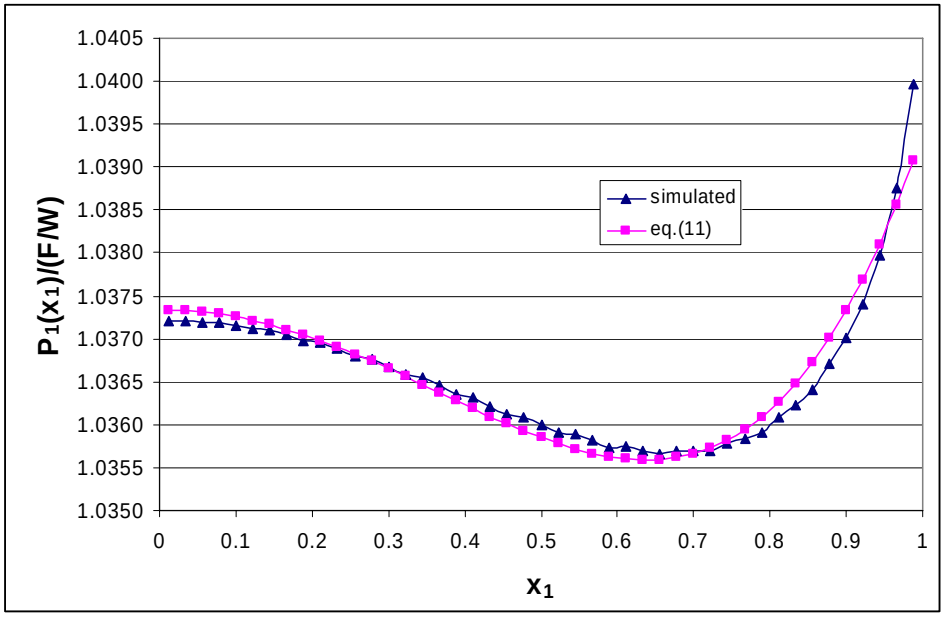

Figure 9. *Comparison of the simulated $P_1(x_1)$ with CROWN426 along the center of the workpiece and to its edge, and approximation of equation (11) of it.*

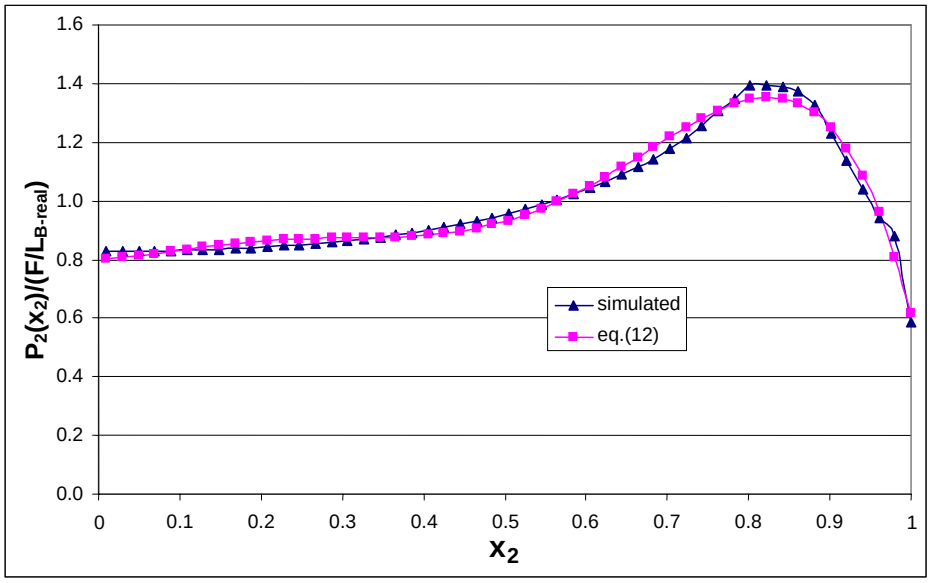

Figure 10. *Comparison of the simulated $P_2(x_2)$ with CROWN426 along the center of the back-up barrel to the end of its contact with the work roll and approximation of equation (12) of it.*